Deep-Sea Research I 79 (2013) 122–140

Contents lists available at SciVerse ScienceDirect

Deep-Sea Research I

journal homepage: www.elsevier.com/locate/dsri

Zooplankton in the eastern tropical north Pacific: Boundary effects of oxygen minimum zone expansion

Karen F. Wishner [a,*], Dawn M. Outram [a], Brad A. Seibel [b], Kendra L. Daly [c], Rebecca L. Williams [a]

[a] Graduate School of Oceanography, University of Rhode Island, 215 South Ferry Rd., Narragansett, RI 02882, USA
[b] College of the Environment and Life Sciences, University of Rhode Island, Kingston, RI 02881, USA
[c] College of Marine Science, University of South Florida, 140 7th Avenue South, St. Petersburg, FL 33701, USA

ARTICLE INFO

Article history:
Received 4 June 2012
Received in revised form
24 April 2013
Accepted 26 May 2013
Available online 3 June 2013

Keywords:
Oxygen minimum zone
Zooplankton biomass
Copepod
Eucalanus inermis
Climate change
Biological pump
Diel vertical migration

ABSTRACT

Oxygen minimum zones (OMZs) may be expanding in their worldwide spatial and vertical extent as a result of global climate change. Here, we highlight structural and functional features of pelagic OMZ zooplankton communities, especially the little known mesopelagic lower oxycline zooplankton assemblage in the eastern tropical north Pacific (ETNP). Day and night vertically-stratified zooplankton samples were collected with a MOCNESS plankton net system to depths of 1000 m during two cruises in 2007 and 2008 as part of the Eastern Tropical Pacific Project. Size-fractionated biomass and selected species distributions were analyzed. A spatial comparison between two stations, Tehuantepec Bowl (TB) and Costa Rica Dome (CRD), with different OMZ thicknesses especially in 2008, was used as a proxy for future potential climate change to show how variability in oxycline depth at the upper and lower OMZ boundaries may have broad consequences for biological distributions and ecosystem function.

The same zooplankton biomass features were present at both locations but responded differently to changes in OMZ thickness and boundary depths. The impact of habitat compression was quantified by the change in proportion of zooplankton biomass in the upper water column. The thermocline was the location of peak zooplankton biomass regardless of OMZ extent. At the lower oxycline, a unique zooplankton assemblage and secondary biomass peak (sharp order of magnitude jump from OMZ core biomass levels) occurred that was strongly associated with a specific oxygen concentration of 2 μM. In 2008, the lower oxycline biomass peak deepened by over 200 m at TB with its expanded OMZ compared to CRD, despite a temperature difference of ~2 °C, while remaining at the same oxygen level. In contrast, another secondary biomass peak corresponding to the daytime depth of diel vertical migration, and occurring within the upper oxycline or OMZ core, was present at the same depth and temperature at both locations, despite different oxygen concentrations. A dense monospecific layer of the copepod *Eucalanus inermis* was sometimes present just above the distinctive more persistent lower oxycline assemblage. While the general ontogenetic migration of this species was previously known, its precise positioning relative to oxygen concentration and the lower oxycline community is a new finding. The vertical re-positioning of biomass layers at the thermocline and lower OMZ boundaries, and the increased depth range of low oxygen water that diel vertical migrators and sinking particles must transit in an expanded OMZ, could have widespread effects on species distributions, the biological pump, and benthic–pelagic coupling.

1. Introduction

Oceanic Oxygen Minimum Zones (OMZs), midwater depth strata with low oxygen concentration and unique zooplankton ecology (e.g. Wishner et al., 2008), may be expanding in their worldwide spatial and vertical extent as a result of global climate change (Stramma et al., 2008; Hofmann and Schellnhuber, 2009; Keeling et al., 2010) or natural climate oscillations (Deutsch et al., 2011). This expansion could have profound effects on oceanic ecosystem structure and function, including species distributions, vertical fluxes, benthic–pelagic coupling, and fisheries (Wishner et al., 1990; Levin, 2003; Diaz and Rosenberg, 2008; Ekau et al., 2010; Rabalais et al., 2010; Stramma et al., 2010; Seibel, 2011). Recent studies highlighted effects of OMZ expansion on habitat use for blue marlin and tunas (Stramma et al., 2011) and longterm changes in the California Current OMZ associated with

---

[*] Corresponding author. Tel.: +1 401874 6402; fax: +1 401874 6523.
E-mail address: kwishner@mail.uri.edu (K.F. Wishner).

0967-0637/$ - see front matter © 2013 Elsevier Ltd. All rights reserved.
http://dx.doi.org/10.1016/j.dsr.2013.05.012

mesopelagic fish abundance (Koslow et al., 2011). “Dead zones” of low oxygen concentration and low biomass occur periodically along the US northwest coast and are due in part to coastal intrusion of the offshore OMZ (Grantham et al., 2004; Chan et al., 2008). OMZs are important in global biogeochemical cycles and the biological pump (e.g. Lam et al., 2009; Kalvelage et al., 2011).

Modern day OMZs are quite extensive (Kamykowski and Zentara, 1990; Morrison et al., 1999; Helly and Levin, 2004; Karstensen et al., 2008), comprising ~8% of global ocean volume (if defined as oxygen $<20\ \mu M$), with the eastern tropical north Pacific (ETNP) being ~41% of global OMZs (Paulmier and Ruiz-Pino, 2009). The interannual El Niño/Southern Oscillation (ENSO) periodically affects the vertical and shoreward extent of low oxygen water in the eastern Pacific, but ecological effects vary with geographic location, depth, and ENSO strength (Arntz et al., 2006; Chavez and Messié, 2009). Multidecadal climate cycles affecting eastern Pacific currents, hydrography, and ecosystems are superimposed on ENSO events (Chavez et al., 2003; Bograd et al., 2008). In past geological eras with warm seas, even more of the ocean was hypoxic or anoxic (Stanley, 2010), situations considered possible endpoints of extreme global warming.

In regions with strong OMZs, the epipelagic habitat is distinctly separated from deeper water by the strong thermocline and oxycline at the base of the mixed layer (coinciding with the upper boundary of the OMZ). While this constrains vertical distributions of many taxa, some zooplankton and nekton show strong diel and ontogenetic vertical migration hundreds of meters into hypoxic water (e.g. Sameoto, 1986; Saltzman and Wishner, 1997a,b; Prince and Goodyear, 2006; Escribano et al., 2009; Maas et al., 2012). These animals have a variety of metabolic and behavioral adaptations for coping with hypoxia (Childress and Seibel, 1998; Rosa and Seibel, 2010; Seibel, 2011, in press; Trueblood and Seibel, in press). Epipelagic and mesopelagic communities also interact as part of the biological pump via the vertical flux and processing of sinking particles (Ducklow et al., 2001; Buesseler et al., 2008), a phenomenon that may be influenced in OMZs by effects of low oxygen on distributions and metabolic processes of zooplankton and nekton.

Within strong OMZs, the steep oxygen gradients (oxyclines) at the upper and lower boundaries create microhabitats of differing oxygen concentration that are characterized by layers of high zooplankton biomass and abundance, with distinct species zonation (Saltzman and Wishner, 1997a,b; Wishner et al., 1995, 1998, 2000, 2008). These characteristics contrast notably with the OMZ core, where oxygen is extremely low but stable, often for hundreds of meters in depth, and where resident zooplankton biomass and abundance are much reduced (Longhurst, 1967; Wishner et al., 1998, 2008; Koppelmann et al., 2005; Smith and Madhupratap, 2005). In locations where the water becomes completely anoxic and sulfidic (Black Sea, Cariaco Basin), metazoan taxa mostly disappear, with some exceptions (Baird et al., 1973; Danovaro et al., 2010; Utne-Palm et al., 2010). However, substantial populations of many taxa penetrate into severely hypoxic OMZ water in diel vertical migration (DVM) or seasonally as part of their life history cycle (e.g. Brinton, 1979; Smith et al., 1998; Hunt and Seibel, 2000; Ashjian et al., 2002; Hidalgo et al., 2005, 2010). Additionally, both the upper and lower OMZ oxyclines, as well as the low oxygen core of the OMZ (and other strong pelagic oxyclines), provide specialized habitats for microbes, including chemoautotrophic groups (e.g. Taylor et al., 2001, 2009; Voss et al., 2001; Molina and Farias, 2009; Ward et al., 2008; Podlaska et al., 2012; Stewart et al., in press; Wakeham et al., 2012). These may provide novel food resources for mesopelagic zooplankton (Gowing and Wishner, 1992, 1998) and a deepwater (non-photosynthetic) source of new production for the biological pump (Taylor et al., 2001; Robinson et al., 2010). Microbial processes, in conjunction with high organic matter input and regional oceanographic circulation limiting midwater oxygen replenishment, are the major drivers creating OMZ biogeochemical gradients (Morrison et al., 1999; Kessler, 2006) that are key environmental structural features affecting zooplankton distributions.

For zooplankton, oxyclines at the upper and lower OMZ boundaries are loci of distributional peaks in the water column, probably also with relatively high rates of trophic processing and biogeochemical transformation (Wishner et al., 1995, 2008). Much of the midwater zooplankton biomass and activity in OMZ regions may be focused within these oxycline boundary communities, in contrast to other mesopelagic regions without strong OMZs (e.g. Steinberg et al., 2008a). If OMZs become thicker or more extensive in the future, the oxycline boundary communities, and the processes they support, may be displaced vertically and horizontally. Boundary-related effects could include altering the depth of zooplankton biomass layers and species distributions and impacting diel vertical migration patterns and life history strategies.

The focus of this paper is to elucidate prominent structural and functional characteristics of pelagic OMZ boundary communities in the ETNP, especially the little known mesopelagic lower oxycline zooplankton community. It also synthesizes broader results from the multidisciplinary Eastern Tropical Pacific Project that investigated ecological and physiological responses of organisms from microbes to squid in the hypoxic habitat and strong oxygen gradients of the ETNP OMZ during 2007–2009. Understanding the ecology of oxycline communities is essential for predicting potential effects of OMZ expansion and illuminating unique vulnerabilities of OMZ zooplankton to climate change. From prior work, we hypothesized that OMZ zooplankton biomass layers would be associated with specific oxyclines, but it was uncertain how other environmental factors, such as temperature and depth, influenced that association. Because most prior studies used broad sampling strata for zooplankton, connections between distributions and oxygen concentration were not well constrained. In this study, narrow sampling strata, along with in situ environmental sensing and serendipitous natural variability between locations and years, provided a unique dataset to separate these influences. We used a spatial comparison between two locations with different OMZ thicknesses as a proxy for temporal change to show how variability in oxycline depth may have broader ecosystem consequences. These two locations were similar to each other in OMZ extent during 2007; however, the OMZ thickness at one station, but not the other, substantially increased in 2008. Biological impacts revealed by the 2008 spatial difference are a theme of this paper.

2. Materials and methods

2.1. Sampling and data collection

2.1.1. Zooplankton

Zooplankton were collected during two cruises to the ETNP. Cruise dates were 18 October–17 November 2007 on the R/V Seward Johnson and 8 December 2008–6 January 2009 on the R/V Knorr. Two stations were intensively sampled for zooplankton along an 8-station north to south transect in oceanic waters west of Mexico and Central America: Station 1, the Tehuantepec Bowl (TB), at 13°N 105°W, and Station 8, the Costa Rica Dome (CRD), at 9°N 90°W (Fig. 1). These stations represented two contrasting productivity regimes (higher productivity at CRD) and had historical records from prior work (Fiedler and Talley, 2006; Fernández-Älamo and Farber-Lorda, 2006; Kessler, 2006; Pennington et al., 2006). The TB site was near locations occupied during the 1980s

VERTEX cruises (Martin et al., 1987), while the CRD has been studied since the 1950s (Fiedler, 2002).

Day and night vertically-stratified samples to 1000 or 1200 m depth were obtained using a 1 m^2 MOCNESS (Multiple Opening-Closing Net and Environmental Sensing System) (Wiebe et al.,1985) with eight 153 μm mesh sampling nets (Table 1). Sampling with net tows involves tradeoffs between the need for consistent depth intervals for geographic or temporal comparisons versus variable depth intervals for feature tracking. We balanced these needs by using standard depth divisions supplemented with targetted narrower strata for selected depth ranges. Zooplankton sampling occurred during the upcast portion of the tow close to noon or midnight. Tows were grouped into 8 or 24-sample vertical profiles. During the 2007 cruise, one 8-stratum “standard” profile to 1200 m was done for biomass at each station day and night. Strata were selected on the basis of initial CTD profiles to encompass key water column zones, but, because of the 8-net limitation of the MOCNESS, strata within the OMZ were each 150 to 300 m thick. For finer resolution of species distributions on the first cruise and for both biomass and species on the second cruise, we did three sets of tows (0–150, 150–550, 550–1000 m) to produce 24-sample vertical profiles. This provided more vertical resolution, especially through the oxyclines. However, not every tow was successful, primarily because of electronic problems. Consequently on the second cruise, we obtained one biomass profile to 550 m and another to 1000 m at each station. However, this did include three sequences from the surface through the OMZ core to the lower oxycline, since that feature was relatively shallow at CRD. Two fine-scale sequences with 25 m thick strata were successfully obtained through the lower oxycline on this cruise. In total, there were 8 biomass profiles to at least 550 m (day and night, both stations, both years), including 6 profiles extending to at least 1000 m and 7 profiles encompassing the lower oxycline, plus additional tows for species information.

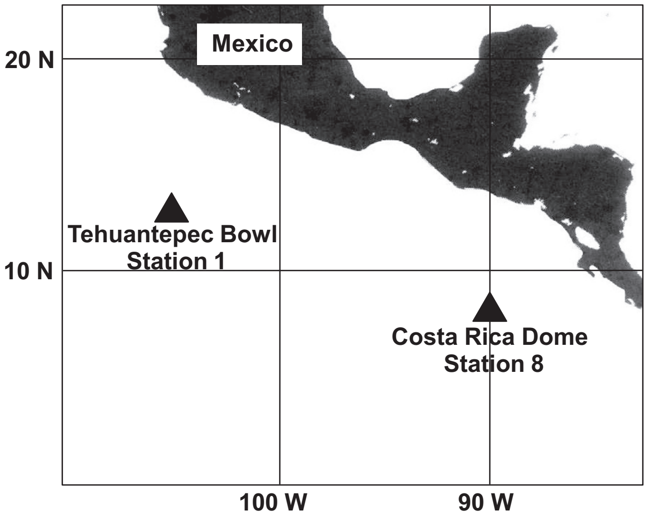

Fig. 1. Map showing MOCNESS sampling locations (triangles).

Profiles to depth were assembled from tows on different dates (Table 1). In two instances, a 25 m missing portion was filled by averaging values from nets above and below. In a few instances, individual nets from other MOCNESS tows were used to fill in gaps. Each of the deeper tows took ~7 h (i.e. most of a day or night centered around noon and midnight) with post-tow net processing plus size-fractionated biomassing requiring an additional ~8 h per tow; these time demands limited the possibility for replicate biomass profiles, given other project needs and wiretime availability. Although compositing of data from different tows is not ideal, it is often done in deep-sea studies and was the only realistic way to obtain high resolution profiles through the deeper OMZ on these multidisciplinary cruises. Patchiness, always a concern in zooplankton distributional studies (Haury et al., 1978), could not be fully addressed because of limited replication; however, the consistent vertical zonation at both locations and on both cruises, and

Table 1
Tow and net interval data. Tow IDs show tows grouped into vertical profiles. The Data column shows information obtained from each series. Abbreviations: B=biomass, S=species abundances, D=day, N=night.

Year and location	Station	Data	Time	Tow IDs	Dates (GMT)	Depth (m)	Net intervals (m) NS=no sample
Oct–Nov 2007							
Tehuantepec Bowl	1	B, S	D	608	28-Oct	0–1200	0–20–80–150–350–550–750–900–1200
Tehuantepec Bowl	1	B	N	609	29-Oct	0–1200	0–20–80–150–350–550–750–900–1200
Costa Rica Dome	8	B	D	614	07-Nov	0–1200	0–20–80–150–350–550–750–900–1200
Costa Rica Dome	8	B	N	621, 622, 617	11, 12, 9-Nov	0–1200	0–20–30–40–50–60–80–100–150–350–550–750–900–1200
Costa Rica Dome	8	B	D	618	09-Nov	0–150	0–20–30–40–50–60–80–100–150
Costa Rica Dome	8	S	D	618, 616, 623	9, 8, 12-Nov	0–775	0–20–30–40–50–60–80–100–150–200–250–300–350–400–450–500–550–575–600–625–650–675–700–733–773
Costa Rica Dome	8	S	N	621, 615, 617, 619	11, 8, 9, 10-Nov	0–1200	0–20–30–40–50–60–80–100–150–200–250–300–350–400–450–500–550–700–750–800–850–900–950–1000–1100–1200
Dec 2008–Jan 2009							
Tehuantepec Bowl	1	B, S	D	626, 630, 631	15, 17, 18-Dec	0–1000	0–20–30–40–50–60–80–100–150–200–250–300–350–400–450–500–550–700–775–800–825–850–875–900–1000
Tehuantepec Bowl	1	B, S	N	633, 628	20, 17-Dec	0–550	0–20–30–40–50–60–80–100–150–200–250–300–350–400–450–500–550
Tehuantepec Bowl	1	S	N	632	19-Dec	550–1000	550–700–775–800–825–851–875–900–1000
Costa Rica Dome	8	B, S	D	635, 637	28, 29-Dec	0–550	0–20–30–40–50–60–80–100–150–200–250–300–350–400–450–500–550
Costa Rica Dome	8	S	D	640	30-Dec	525–1000	525–550–575–600–625–650–750–900–1000
Costa Rica Dome	8	B, S	N	638, 641, 636	30-Dec, 1-Jan, 29-Dec	0–1000	0–20–30–40–50–60–80–100–150-NS-200–250–300–350–400–450–500-NS-525–550–575–600–625–650–750–900–1000

the comparative differences between locations, provided a solid basis for logical interpretations about biomass boundary layers.

Biomass processing generally followed protocols from the Joint Global Ocean Flux Study (JGOFS) and Zooplankton Methodology Manual (Wishner et al., 1998; Postel et al., 2000). Cod ends were placed in buckets with plastic ice packs immediately upon retrieval to keep zooplankton cool in the tropical environment as an aid to preservation. Samples were rinsed from nets and cod ends with filtered seawater into 153 μm metal sieves and photographed. Samples were then split with a flat-bottomed Motoda splitter. Half the sample was preserved in 4% sodium-borate-buffered formalin for distributional studies, 1/4 was processed for size-fractionated biomass, and 1/4 was refrigerated for microscopical and stable isotope processing. For size-fractionated biomass, the sample split was poured through a stacked series of nitex mesh sieves (meshes of 5, 2, 1, 0.5, and 0.2 mm) using filtered seawater; then the contents of each sieve were poured onto pre-weighed 48 mm diameter circles of nitex mesh (200 μm) and rinsed with de-ionized water. In some cases with larger samples, the catch was split further or multiple filters were used for a single sample. At least two blanks (filters processed as above but with no sample) were prepared for each tow. Nitex circles were folded, wrapped in aluminum foil, and dried to 60 °C in a drying oven at sea for a minimum of 48 h, then stored in desiccators. After the cruise, samples were dried again to 60 °C in the lab and weighed on a Cahn ATI microbalance to obtain dry mass (mg). The term "zooplankton" in this paper refers to animals >153 μm in size caught in the MOCNESS, including both mesozooplankton and micronekton; "zooplankton biomass" includes those >200 μm.

For several samples from TB in 2007 when gelatinous abundance was high, displacement volume measurements were made at sea by placing large gelatinous animals into a graduated cylinder. Displacement volume was converted to mg dry mass using equations in Postel et al. (2000), their Table 4.7. A conversion range for mg dry mass (mg wet mass)$^{-1}$ of 0.035–0.05 was listed; we used the mean of 0.0425 and the assumption that 1 mL displacement volume = 1 g wet mass. We note these measurements separately from the regular dry mass results to document the presence of a gelatinous layer while recognizing that its biomass remains uncertain.

Large taxa were counted from the entire preserved portion before splitting, while abundances of smaller taxa were obtained from splits of the remaining fraction. Copepods were the focus for species analysis, with a target count of 100–200 calanoid copepods per sample (from a list of selected species); this required sample splits of 1/8 to 1/512. Calanoid copepods were identified to species and life history stage when possible, using a Wild dissecting microscope, supplemented with observations from an Olympus compound microscope. Total copepod abundances, abundances of small miscellaneous taxa, and the ratio of calanoids to noncalanoids were obtained from subsequent counts of aliquots (using a Stempel pipette) of the same split. Copepod distributions were obtained from day and night vertical profiles to depth at CRD in 2007 and from 0 to 200 m at TB in 2008 (Table 1). Copepods from the family Eucalanidae were counted to depth at both stations both years. For this paper, only a few examples of species distributions are shown; more comprehensive analyses will be presented elsewhere.

Biomass and abundance data were converted to concentration (mg/m^3 or number/m^3, respectively) by dividing by the water volume filtered by the net, after accounting for split or aliquot size. Total abundances for each taxon were obtained from the sum of results of the several counting procedures described above. For water column biomass or abundance (per m^2) for selected depth intervals, concentration within a net was multiplied by the thickness of that depth interval, and values from successive intervals were summed for that depth range. "Water column biomass" comparisons encompassed the depth range from 0 to 1000 m in 2007 but only 0–550 m in 2008, because of sampling problems with some deep profiles. Biomass was converted to carbon equivalents (mM carbon/m^3) using the equation of Wiebe et al (1975) (see also Wiebe, 1988; Postel et al., 2000), namely mM carbon = 10^((log$_{10}$(mg dry mass)−0.499)/0.991)/12.01. This was identical to calculations in Wishner et al. (1998) for the Arabian Sea JGOFS and enabled direct comparisons between these two OMZ regions.

Vertical profiles of zooplankton δ^{15}N stable isotope values from some MOCNESS samples were compared to vertical profiles of zooplankton biomass from the same samples to highlight an intriguing phenomenon at the lower oxycline. Methods will be described in detail in an extensive analysis in progress of vertical patterns of δ^{13}C and δ^{15}N stable isotopes of zooplankton and particles through the OMZ. Briefly, for the data shown in this paper, 1/4 splits of fresh zooplankton samples from the biomass tows were size fractionated into four size classes (0.2–0.5, 0.5–1, 1–2, 2–5 mm), with subsamples frozen at sea. In the lab, samples were dried at 70 °C, ground to a fine powder, and measured for δ^{15}N using a Carlo-Erba NA 1500 Series II Elemental Analyzer interfaced to a Micromass Optima Isotope Ratio Mass Spectrometer. The δ^{15}N isotope value for zooplankton from each net is the biomass-weighted mean of the four size classes, each size class isotope value being the mean of four subsamples.

2.1.2. Environmental data

Hydrographic profiles used here were obtained by MOCNESS sensors, supplemented by CTD data if there were MOCNESS electronic problems. MOCNESS upcast values were used when available, since those were simultaneous with plankton collection. MOCNESS sensors included temperature (SBE 3P-1), conductivity (SBE 4C-1), fluorescence (Seapoint chlorophyll fluorometer), light transmission (Wetlabs CST-667DR 25 cm beam transmissometer), oxygen (SBE 43-1), pressure (depth), and volume filtered. Salinity and oxygen used pumped systems in 2008; only salinity was pumped in 2007. MOCNESS hydrographic data were recorded every 4 s. Sensors were calibrated by the manufacturer before the cruise and by measurements of selected CTD/rosette water samples (microWinkler procedure for oxygen).

Different units of the same Sea-Bird oxygen sensor model (SBE 43) were used on the CTD, MOCNESS, and a towed camera system. Sea-Bird electronic oxygen sensors were used, rather than optodes, because of the need for rapid-response profiling data. Resolution of both Sea-Bird and Winkler measurements is ~0.02 mL/L, and values from the different SBE 43 instruments varied by similar amounts for the lowest oxygen water of the OMZ core (which we assumed remained constant). A 2008 calibration exercise suggested the possibility that CTD Sea-Bird values that year might be adjusted 27% higher. Additionally, there was substantial small-scale variability between tows, days, and stations in oxygen profiles through the upper oxycline, likely representing short-term oxygen intrusions. The MOCNESS oxygen sensor did not always record realistic values near the air-sea interface. Because of these issues, we did not attempt an overall multi-cruise convergence of oxygen measurements from the different instruments and years and have used MOCNESS sensor values obtained simultaneously with the zooplankton samples whenever possible. However, precise oxygen values, especially for the lowest oxygen levels, remain uncertain for reasons noted above.

Real-time profiles of temperature, salinity, light transmission, and oxygen available on the shipboard MOCNESS tow computer enabled adaptive sampling at oxyclines. Experience showed that the oxygen inflection point at the base of the OMZ core (start of the lower oxycline) was usually associated with a particle peak in transmissometer data, and this corresponded to the presence of a unique lower oxycline zooplankton community and relatively high biomass layer. We targeted this biomass layer by noting these features on the downcast and selecting appropriate depth strata for the upcast sampling portion of some tows. In contrast to CTD casts with vertical speeds ~50 m/min, the MOCNESS was towed along an oblique path with a vertical speed at the deeper depths of only 1–3 m/min. Each deep net filtered ~600 to $>1000\ \mathrm{m}^3$ (maximum $2270\ \mathrm{m}^3$) of water and required about 20–25 min of towing at 1.5–2 kt. Smaller volumes were filtered for upper nets, with more rapid vertical speeds. These long times at depth and slow crossing of oxygen gradients allowed us to visualize particle peaks as clouds in transmissometer data, enabled the oxygen sensor to stabilize at low oxygen values, and highlighted small-scale variability of oxygen intrusions at oxyclines. Obtaining simultaneous oxygen and zooplankton data through these gradients was essential; profiles from CTD casts or MOCNESS two hours or days earlier were not always an accurate representation of the water column during plankton collection.

2.2. *Data analyses*

Hydrographic data were processed by removing outliers and binning within 1 m intervals. Three-point running means were used to smooth transmissometer and fluorescence data. Mean values of processed hydrographic data encompassing the depth range of each net were calculated. Statistical and graphical analyses were performed with Microsoft Excel, Statistica, and Primer v6 software (Clarke and Gorley, 2001). Patterns of zooplankton community size structure were analyzed using Bray-Curtis cluster analyses based on size fraction biomasses within samples. Size fraction dry masses were square-root transformed, and sample clusters were arbitrarily defined at the 63% similarity level to produce meaningful assemblages. *A priori* factors tested for significance included ecological zone, depth zone, station, year, and day–night (definitions below and in Table 2). ANOSIM and SIMPER tests quantified similarities and dissimilarities within and between groups. Sign tests were used to compare total biomass depth zone profiles between stations within years, between years at the same station, and between paired day and night profiles.

3. Results

3.1. *Ecological zones of the OMZ*

To understand OMZ biology, it is essential to understand OMZ physical and ecological zonation. Ecological zones of the OMZ, defined originally from the Arabian Sea (Wishner et al., 2008), form a vertical series of unique habitats with different zooplankton, oxygen, predators, and food. This perspective provides a useful framework for the ETNP as well. Fig. 2 shows hydrographic profiles with labelled ecological zones; Table 2 lists zonal depth ranges by station and year. Zonal depths are location-specific and related to profile shape. For MOCNESS-based zooplankton data, zonal ranges, based on definitions below, were rounded to the nearest MOCNESS net division depth (Table 1) after isolating the

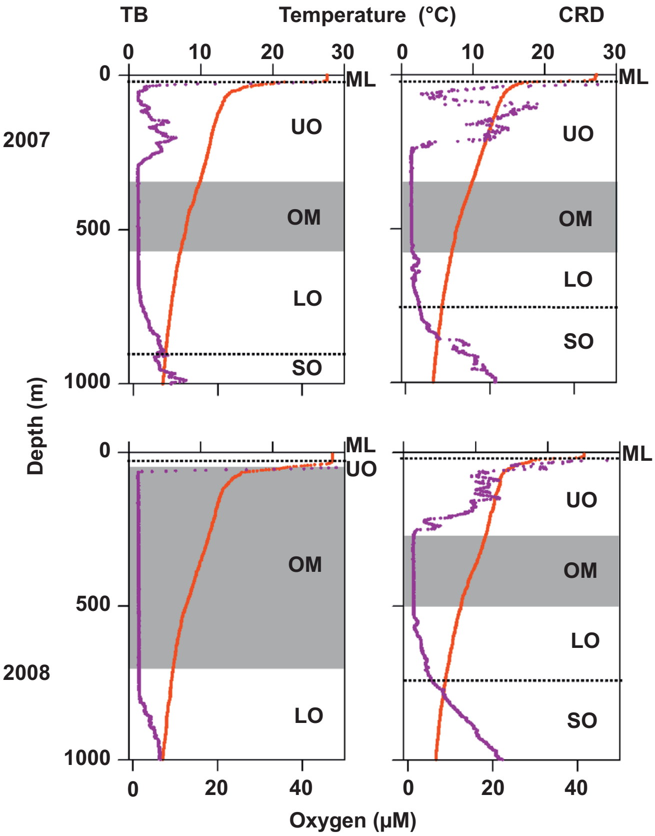

Fig. 2. Vertical profiles of temperature and oxygen from each station each year (tows 609, 614, 632, 636). Left graphs are from station TB and right graphs are from station CRD; top row is from 2007 and bottom row is from 2008. Labels and dashed lines denote ecological zones (see Table 2 for zonal abbreviations and depth ranges). The gray box marks the OMZ core (OM); its upper and lower boundaries are 1.8 μM oxygen (0.04 mL/L). The oxygen zero point is offset slightly to the right for clarity, and oxygen values in the mixed layer extend offscale to 147 μM.

Table 2
Depth intervals comprising ecological zones and depth zones at each station each year. Abbreviations are below each name. Depths were rounded to net sampling divisions. For CRD in 2007, the LO boundary was based on net intervals from biomass sampling (Table 1) (the next deeper biomass net extended over a broad depth range from 750 to 900 m). A finer scale tow used only for species abundances (Tow 619) showed the LO extending to 800 m based on oxygen values, but, for consistency among tows, 750 m was used for this boundary.

Location	**Depth intervals for ecological zones (m)**					
	Mixed layer ML	**Upper oxycline UO**	**OMZ core OM**	**Lower oxycline LO**	**Suboxycline SO**	**Comments**
2007						
TB (Sta. 1)	0–20	20–350	350–550	550–900	900–1200	UO-A=20–150, UO-B=150–350, SO used to 1000 m only
CRD (Sta. 8)	0–20	20–350	350–550	550–750	750–1200	UO-A=20–150, UO-B=150–350, SO used to 1000 m only
2008						
TB (Sta. 1)	0–40	40–80	80–700	700–1000	Below tows	
CRD (Sta. 8)	0–20	20–300	300–500	500–750	750–1000	UO-A=20–150, UO-B=150–300
	Depth Zones (m)					
	Upper	**Mid**	**Deep**			
All locations	0–150	150–550	550–1000			

OMZ core samples as those entirely within the lowest oxygen water, representing the most extreme habitat. Samples from depth strata that included any higher oxygen water were assigned to the oxyclines (or other) zones described below.

The Mixed Layer (ML), the epipelagic water column above the thermocline, was thin with oxygen approaching air saturation. The shallow thermocline in this tropical region was abrupt, with a temperature change from ~25–28 °C in the ML to ~15–18 °C at the start of the upper oxycline (only 20–40 m depth) and ~10–12 °C at its base (250–350 m). The thermocline also was coincident with a sharp drop in oxygen, marking the top boundary of the OMZ's Upper Oxycline (UO). Although the UO was characterized by generally declining oxygen concentrations, it often included spatially and temporally variable oxygen intrusions. Where the UO depth range was broad, it was subdivided into two sections: UO-A (thermocline to 150 m) and UO-B (150 to either 300 or 350 m, i.e. the start of the OMZ Core). The OMZ Core (OM) had the lowest oxygen values with relatively little change vertically. In the region of our study, OM oxygen concentration (MOCNESS sensor) was ~1.8 μM (0.04 mL/L) so this value, along with the depths of the upper and lower inflection points in vertical oxygen profiles, was used to define OM boundaries. At the lower oxycline (LO), oxygen concentration began to increase with depth while temperature, salinity, and density continued their gradual depth-associated trends (in contrast to the abrupt density step at the thermocline). As described in detail later, the LO was the location of a secondary zooplankton biomass and multispecies abundance peak, some taxa limited to this zone. Below the LO in the Suboxycline (SO), oxygen continued to increase with depth, but the faunal composition shifted to typical bathypelagic taxa. The division between the LO and SO was arbitrarily defined in our dataset as an oxygen concentration of 9 μM (0.2 mL/L) to correspond with net sampling strata. Oxygen was still increasing with depth at the lower limit of sampling. To clarify terminology used in this paper, "OMZ" refers generally to the full extent of the midwater low oxygen habitat (combined UO, OM, LO, and SO), LO is the lower part of the OMZ where oxygen begins to increase with depth, and "LO layer" or "LO community" is the presumably thinner zone of high biomass and abundance that occurs within the LO.

A pictorial demonstration of faunal composition and taxonomic shifts through these ecological zones pairs day and night photographs of whole fresh MOCNESS samples from each zone (Fig. 3). Key features are the deep penetration of diel vertical migrators (fish and euphausiids) during the day into the UO and OM and their shallower occurrence or complete absence from these zones at night. The sparseness of zooplankton in the OM compared to the higher abundances in the UO and LO is apparent, as is the taxonomic shift between the LO and SO. The ML had high abundances day and night. These features are documented quantitatively below.

3.2. Overall biomass trends

There were strong spatial and temporal patterns in water column zooplankton biomass between stations and years, based on comparisons of paired day or night profiles (Tables 3 and 4A). CRD was a significantly richer habitat than TB during both years ($p=0.03$ for all sign tests). Total CRD biomass was ~3 × higher than TB biomass in 2007 and 1–2 × higher than TB in 2008 for both the 0–1000 m and 0–550 m water column ranges. However, the 2–5 mm size class was consistently 8–9 × higher in biomass at CRD versus TB (both years, most zones, Table 4A). Biomass in 2008 was significantly greater than that in 2007 ($p=0.03$ for all sign tests), by ~3 × at TB and 1.5 × at CRD.

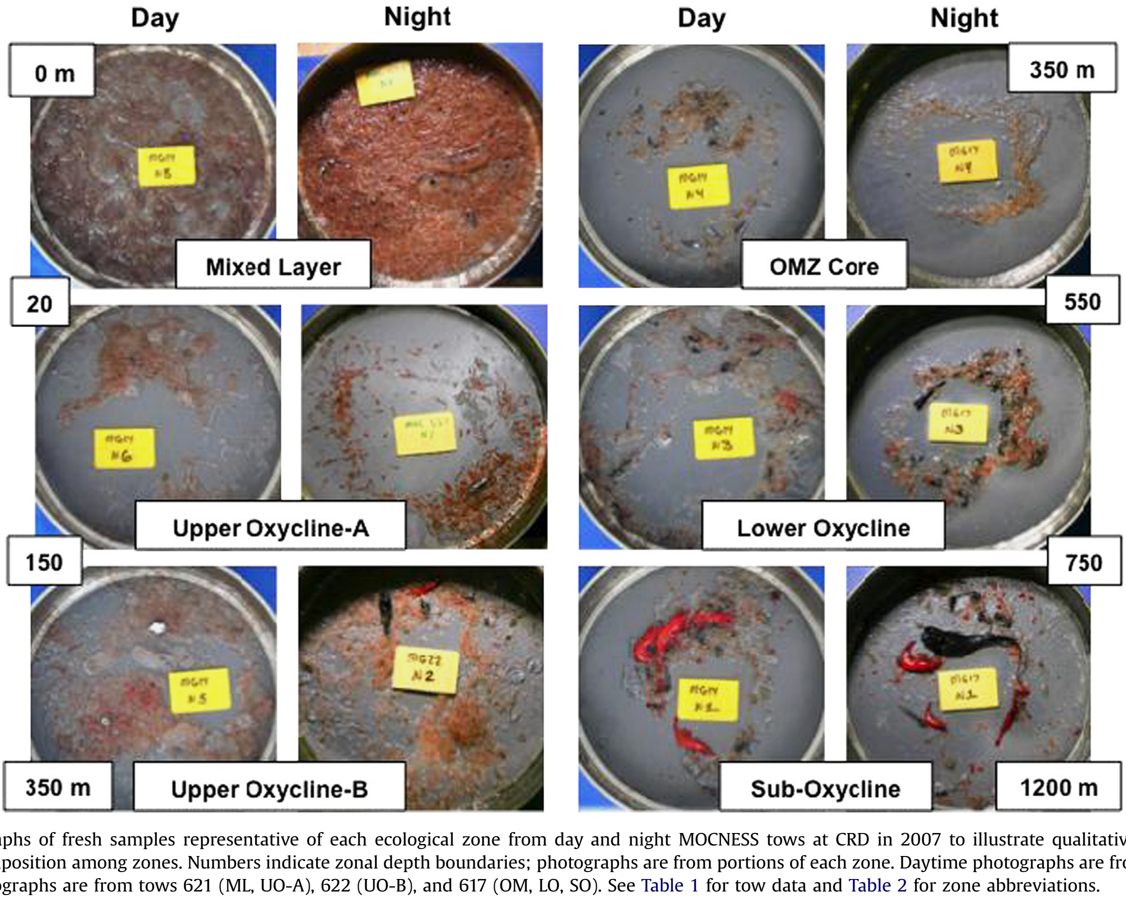

Fig. 3. Photographs of fresh samples representative of each ecological zone from day and night MOCNESS tows at CRD in 2007 to illustrate qualitative differences in community composition among zones. Numbers indicate zonal depth boundaries; photographs are from portions of each zone. Daytime photographs are from tow 614, and nighttime photographs are from tows 621 (ML, UO-A), 622 (UO-B), and 617 (OM, LO, SO). See Table 1 for tow data and Table 2 for zone abbreviations.

Table 3
Biomass totals (sum of dry mass of all size fractions) for ecological zones (see Table 2 for ecological zone depth ranges) and standard depth intervals. Biomass of large gelatinous organisms, not included in size fraction totals, is at the bottom. NA=not available, usually because depth range of interval exceeded tow depth.

Yr–station	**Ecological zone or depth range**									
Day or night	**0–1000 m** mMC/m^2	**0–1000 m** mg/m^2	**ML** mg/m^2	**UO** mg/m^2	**OM** mg/m^2	**LO** mg/m^2	**SO** mg/m^2	**0–150 m** mg/m^2	**150–550 m** mg/m^2	**550–1000 m** mg/m^2
2007 TB										
D	39	1386	289	624	135	214	124	759	290	338
N	34	1214	363	715	20	63	53	990	108	115
2007 CRD										
D	118	4177	709	2419	224	245	580	2131	1221	825
N	113	4000	671	2783	123	229	194	3062	515	423
2008 TB										
D	93	3314	767	1486	647	415	Below tow	2334	518	462
N	NA	NA	956	2017	599	NA	Below tow	3169	258	NA
2008 CRD										
D	NA	NA	676	4259	305	627	NA	3152	2715	NA
N	145	5135	597	2812	125	1146	454	2708	1531	896
Gelatinous										
2007 TB N			472	540						
2007 CRD D			2408	6270						

A large gelatinous component occurred twice in 2007, in a TB night tow (609) and CRD day tow (614) (Table 3). Salps comprised the TB patch, while ctenophores, both lobate and *Beroe* spp., comprised the CRD patch. Gelatinous animals occurred in the two upper nets (0–80 m), which included the ML, thermocline, and part of the UO. Other nets, especially in 2007, contained remnants of unidentifiable gelatinous organisms.

Water column total dry weight biomass was similar between day and night profiles (Table 3, sign tests not significant), indicating little differential net avoidance between day and night overall and supporting the use of day versus night comparisons in tracking vertical migration. The day to night ratio of total water column biomass between paired profiles was ~1 (range: 0.8–1.4) for both 0–1000 m and 0–550 m depth ranges, although day/night ratios showed more variability (range: 0.3–2.7) for individual size classes, especially the largest.

3.3. *Zonal size class composition*

Zooplankton community size structure varied among ecological zones, as shown by the proportionate composition by size fraction within each zone (Fig. 4, Table 4A). Shallow zone communities were dominated by smaller size classes, while the deepest zones were dominated by larger-sized taxa. For example, in the ML and UO, each of the two smallest size classes comprised 5–36% of zonal biomass (sum of both classes within a profile = 10–57%) compared to the two deepest zones, where each of these size classes comprised only 1–8% of zonal biomass. In the SO, the >5 mm size class represented 51–88% of total zonal biomass but was proportionately less important shallower.

Diel shifts occurred in size class composition within the different zones (Fig. 4, Table 4A). The UO was co-dominated by two intermediate size classes (1–5 mm), but with a diel input at night from large animals ascending from depth. Large diel vertical migrators were also evident in the ML at night. The largest diel shift in size class composition occurred within the OM. There, the most common size classes at night were the intermediate 1–2 mm and 2–5 mm groups (each representing 13–61% of total biomass), but during the day, the influx of large (>5 mm) diel vertical migrators descending from above accounted for 12–67% of total OM biomass. The LO was dominated day and night by the three largest size classes (>1 mm). In contrast to other ecological zones, LO size composition was similar day and night, suggesting no DVM by most of these organisms.

3.4. *Vertical distribution of biomass and size classes*

The vertical structure of zooplankton biomass showed distinctive features associated with OMZ hydrographic structure (Fig. 5, Table 4B). The highest biomass occurred in a narrow band within the thermocline (top of the UO). This was generally a 10 m thick interval (representing a single net in a profile), usually at 20–30 m depth, except for TB in 2008, when the thermocline was deeper and the biomass peak occurred at 50–60 or 60–80 m. The upper and lower boundaries of the OMZ core were characterized by secondary zooplankton biomass peaks day and night, delineated by the finer-scale midwater sampling in 2008. The biomass peak at the upper OMZ core boundary (base of the UO) was especially prominent in 2008 at CRD from 200 to 250 m. At the LO, a distinct zooplankton layer occurred, producing an abrupt order of magnitude jump in biomass compared to the sparse OMZ core just above (Fig. 5). In 2008, the LO biomass peak occurred at 775–800 m at TB and 525–550 m at CRD. The center of this secondary peak was probably narrower than our 25 m sampling interval, but its effects extended for about 50–75 m (two to three net intervals in the fine scale sampling).

The percentage of water column biomass within each ecological and depth zone varied with size class (Fig. 6, Table 4A). Most of the water column biomass of smaller zooplankton, dominated by copepods, occurred at shallower depths day and night compared to the broader, deeper, and daily variable vertical positioning of larger animal biomass. The most obvious feature was the high percent of water column biomass of the two smallest size classes that was restricted to the ML plus UO ecological zones (mean of 85% ± 9, $n=12$) and the 0–150 m depth range (mean of 80% ± 8, $n=12$) during both day and night. These small zooplankton have minimal presence in the OM (mean percent of water column biomass of 4% ± 2, $n=10$) except for TB in 2008, discussed later. The LO stood out for most size classes and tows as a zone of higher biomass percent than the OM region just above. In contrast, the

Table 4
Biomass summaries. See Table 2 for depth ranges and ecological zone abbreviations. NA=not available. (A) Biomass of each size fraction within each ecological and depth zone for both stations and years. Daytime data are in the left set of columns and night data in the right set of columns. (B) Biomass (sum of all size fractions) for individual nets representing selected maxima and minima of vertical biomass profiles. Data are from 2008 when finer-scaled sampling occurred. TH=thermocline. The DVM net was determined from day data, and the net from the same depth range is shown for the night comparison. For the OM, the mean of two nets (400–450, 450–500 m) was used to document minimum biomass.

A.		**Size fraction biomass-day (mg/m^2)**					**Size fraction biomass-night (mg/m^2)**				
Yr–station	**Zone**	**>5 mm**	**2–5 mm**	**1–2 mm**	**0.5–1 mm**	**0.2–0.5 mm**	**>5 mm**	**2–5 mm**	**1–2 mm**	**0.5–1 mm**	**0.2–0.5 mm**
2007 TB	ML	0.0	12.6	126.3	77.2	72.7	0.0	40.3	133.2	109.3	80.2
	UO	20.4	133.7	184.8	137.2	148.1	63.5	94.1	256.9	119.1	181.3
	OM	90.1	19.0	14.3	4.4	7.4	0.0	8.8	3.4	4.7	3.2
	LO	111.5	20.3	51.2	17.9	13.2	26.8	9.2	15.3	6.8	4.6
	SO	109.1	5.6	4.6	2.2	2.1	34.7	4.5	8.4	2.5	2.6
	0–150 m	3.7	88.3	259.4	198.7	208.4	12.1	121.6	376.0	223.4	256.5
	150–550 m	106.8	76.9	66.1	20.0	19.7	51.4	21.6	17.5	9.7	8.3
	550–1000 m	220.7	25.9	55.9	20.1	15.3	61.4	13.7	23.7	9.3	7.2
2007 CRD	ML	0.0	173.1	278.4	150.0	107.5	121.2	180.1	174.9	109.8	85.1
	UO	307.8	1115.7	519.7	224.6	251.2	1220.7	1002.2	287.9	141.5	130.3
	OM	113.1	65.3	18.5	13.3	13.7	0.0	75.0	22.1	11.3	14.6
	LO	62.8	89.2	69.4	15.6	8.4	53.0	86.3	57.9	19.7	12.5
	SO	450.1	53.8	41.8	19.8	14.4	98.9	40.2	26.7	15.2	12.7
	0–150 m	69.8	761.9	653.6	320.9	324.8	1318.3	899.9	428.7	220.6	194.4
	150–550 m	351.2	592.2	162.9	67.0	47.6	23.7	357.4	56.2	42.0	35.6
	550–1000 m	512.8	143.0	111.2	35.4	22.8	151.9	126.5	84.6	34.8	25.2
2008 TB	ML	0.0	16.3	314.4	277.2	158.6	44.2	130.3	278.3	306.9	196.0
	UO	93.1	144.1	787.2	239.8	221.5	60.4	480.3	780.0	253.5	443.0
	OM	76.9	143.5	203.5	81.2	141.7	25.0	81.7	185.9	117.6	188.5
	LO	119.5	193.3	53.2	23.9	24.8	NA	NA	NA	NA	NA
	SO	Below tow	Below tow	Below tow	Below tow	Below tow	Below tow	Below tow	Below tow	Below tow	Below tow
	0–150 m	98.4	162.5	1136.3	534.5	402.0	110.7	657.1	1137.5	589.4	674.1
	150–550 m	71.6	134.8	154.9	55.1	101.2	12.8	15.4	61.8	60.0	107.8
	550–1000 m	119.5	199.8	67.1	32.4	43.5	NA	NA	NA	NA	NA
2008 CRD	ML	0.0	272.6	176.6	149.3	77.2	35.3	284.7	134.8	82.1	60.2
	UO	534.3	1957.1	731.3	527.7	509.0	301.9	1105.4	670.5	378.4	356.0
	OM	100.8	133.5	29.0	14.4	26.8	0.9	61.3	16.7	14.0	32.5
	LO	55.1	532.3	27.2	5.2	7.4	165.0	843.7	79.4	30.6	26.8
	SO	NA	NA	NA	NA	NA	326.6	68.3	29.4	13.4	16.8
	0–150 m	33.0	1314.8	752.2	540.9	511.2	261.9	1009.5	728.9	350.2	357.8
	150–550 m	657.2	1580.7	212.0	155.7	109.1	94.2	1073.4	130.0	133.8	99.1
	550–1000 m	NA	NA	NA	NA	NA	473.5	280.5	71.9	34.4	35.5

B.	**Biomass features (mg/m^3) and associated net depth range (m)**							
Station	**TH Max**	**Depth**	**DVM Max**	**Depth**	**OM Min**	**Depth**	**LO Max**	**Depth**
TB-Day	81.5	50–60	2.3	250–300	0.7	400–500	5.3	775–800
TB-Night	65.1	60–80	0.7	250–300	0.3	400–500	NA	
CRD-Day	92.8	20–30	19.4	200–250	1.1	400–500	NA	
CRD-Night	101.4	20–30	5.6	200–250	0.4	400–500	18.7	525–550

largest size class, dominated by fish and shrimp, showed a much broader water column biomass distribution and a large diel shift in dominant zone of occurrence. During the day, the majority of the largest size fraction water column biomass occurred in the 550–1000 m depth range (54% ± 13, $n=3$) and in the OM to SO ecological zones (76% ± 15, $n=3$). At night, much of this biomass moved into the UO and ML.

3.5. Diel vertical migration (DVM)

A strong signal of DVM, undertaken especially by larger size classes, was evident in comparisons of percent biomass change (night minus day) within each ecological and depth interval (Table 5). Large size classes moved from depth during the day into the upper 150 m, as shown by large positive values of % biomass change (35 ± 28, range: 3–81). Euphausiids, abundant in the 2–5 mm size class, and myctophid fish, part of the largest size class, were major components. Smaller size classes had much more restricted DVM primarily within the upper 150 m, with % change small and variably positive or negative. Below 150 m, the largest two size classes had mostly negative biomass changes (−69 to 9%, all but 1 value negative) reflecting their strong daytime descent to depth, while the two smallest size classes once again hovered around 0 indicating minimal deep DVM. The logarithmic depiction of biomass (see spatial comparison discussed later) highlights the increase in total midwater biomass during the day versus the night; diel differences in vertical and zonal percentage composition, described earlier, also support these DVM patterns (Figs. 4 and 6).

3.6. Biomass sample groups based on size structure composition

Cluster analyses using zooplankton community size structure identified five major groups of samples plus two smaller groups. Samples within a group had similar biomass size structure composition, and sample groups were associated with pertinent environmental features. Average similarities within groups ranged from 73 to 81% and significant average dissimilarities between groups from 38 to 87% (Table 6). The *a priori* factors of ecological zone, depth zone, and station showed significant average

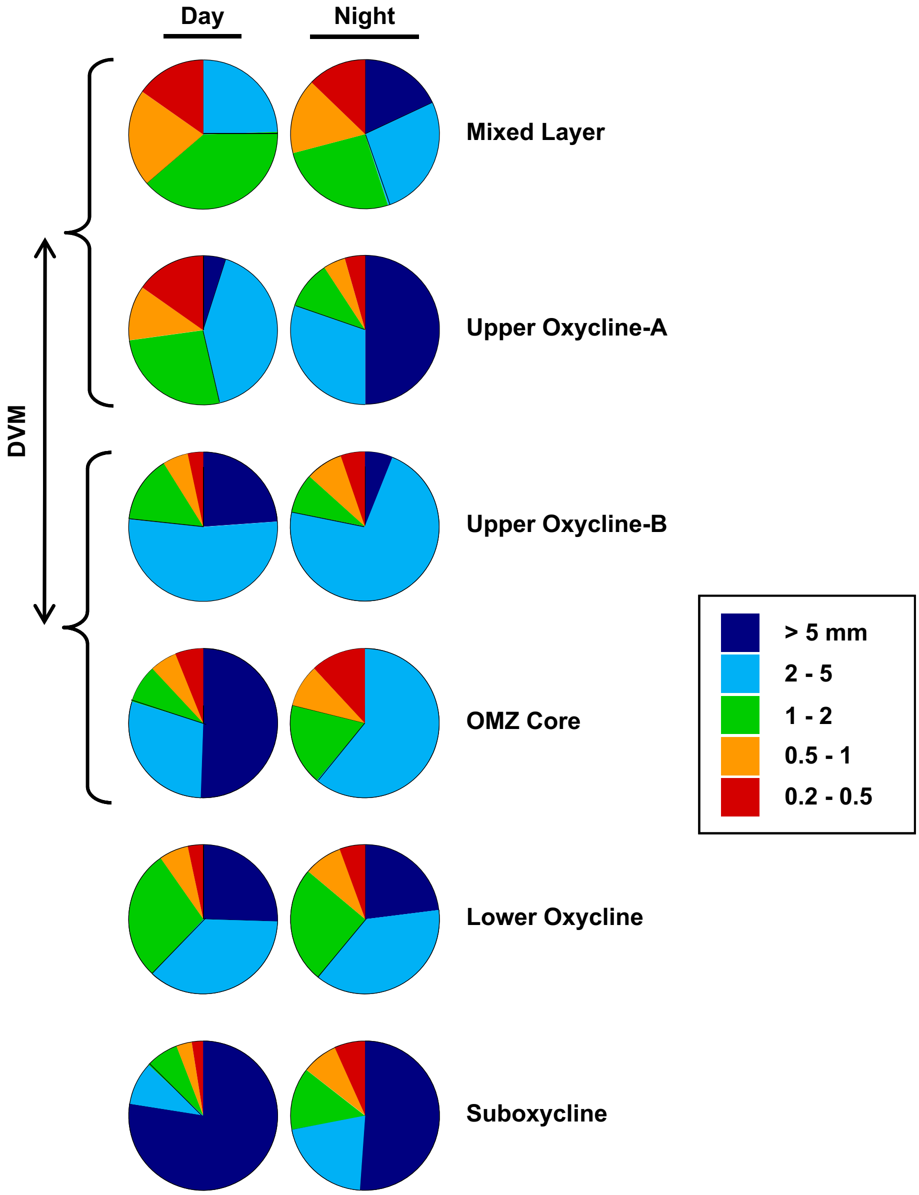

Fig. 4. Proportionate composition day (left) and night (right) by size class within each ecological zone (CRD, 2007). Diel vertical migration (DVM) between zones, particularly prominent for the two largest size classes, is indicated by the arrow.

dissimilarities among groups, but the factors of year and day–night were not significant.

3.7. *Species distributions*

Vertical distributions of zooplankton species interacted with OMZ hydrographic structure. Details of taxonomic distributions will be presented in other papers; here, selected examples are shown to illuminate biomass patterns. Copepods included species limited to the ML and thermocline, upper and lower OMZ oxyclines, or SO (Fig. 7). Distributions of different species were associated with different depths and oxygen concentrations. The vertically distinct distributions of congeneric species of the copepod genus *Lucicutia* suggested niche separation even among closely related taxa. DVM occurred to different depths for different species and taxa, resulting in daytime layers within the UO and OM (Fig. 8). Euphausiids migrated primarily between shallower and deeper parts of the broad UO, while myctophids showed DVM well into the lowest oxygen OM water. Copepod DVM was generally limited to the upper 150 or 300 m.

3.8. *Lower oxycline (LO) community*

The LO was characterized by a sharp secondary peak (order of magnitude jump) in zooplankton biomass and abundance compared to the OM and SO (Fig. 5). The LO zooplankton peak was the result of two superimposed phenomena: a partly endemic multispecies assemblage, termed the “LO community”, that was present in all LO tows, and an occasional (probably seasonal) monospecific aggregation of certain life history stages of the copepod *Eucalanus inermis* that occurred slightly shallower at some locations and times (Fig. 9). Although in some tows, these two layers overlapped within the same net, other tows clearly separated the layers into adjacent 25 m sampling intervals (Table 7).

The depth of the LO community varied with OMZ thickness but was consistently associated with a specific oxygen concentration and the inflection point of the vertical oxygen profile. The LO

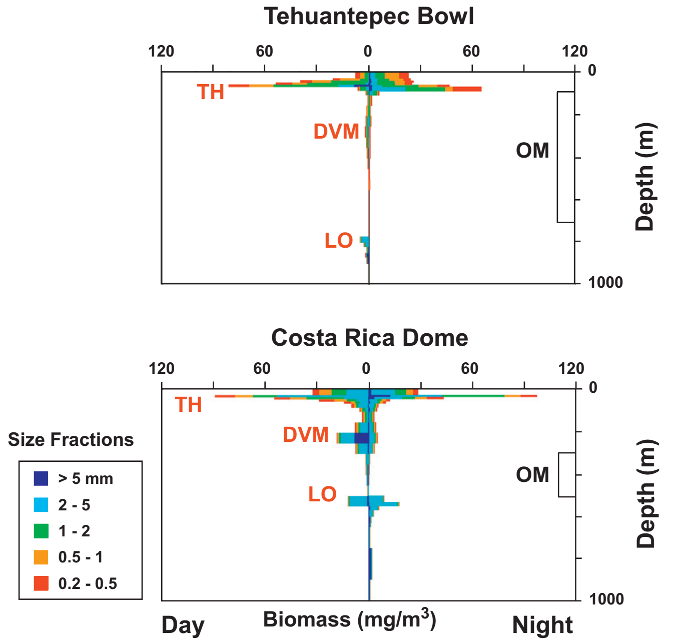

Fig. 5. Day (left) and night (right) size-fractionated zooplankton biomass profiles (0—1000 m) at the two stations in 2008. The box labeled OM marks the depth range of the OMZ core at that station. Biomass peaks at the thermocline (TH), daytime depth of vertical migration (DVM), and lower oxycline (LO) are labelled (see Table 4B for values of these biomass features). Deep biomass values are missing for night at Tehuantepec Bowl and day at Costa Rica Dome (see Table 1 for net depth intervals). These linear scale plots make an interesting visual comparison to vertical biomass profiles from the subtropical and subarctic Pacific (Steinberg et al., 2008a, their Fig. 1); note that biomass axes and net strata differ between the two studies. Total biomass plotted on a logarithmic axis, that highlights DVM and layer depth shifts, is shown later.

community abundance peak occurred at 575–600 m at CRD both years and at 800–825 m at TB in 2008, at an oxygen concentration of ~2 μM (0.045 mL/L) in all cases (Table 7). The precise oxygen value has some uncertainty (see methods) and covers the depth range of a net interval, but it was consistently slightly higher than the OM value. As discussed later, between-station spatial variability in LO layer depth in 2008 was used as a proxy for impacts of potential future OMZ expansion.

The ETNP LO community was a unique multispecies assemblage with characteristic copepods, shrimp, and fish, similar to that previously described from the Arabian Sea (Wishner et al., 2000, 2008). A key visually-prominent indicator species was the bright orange calanoid copepod *Lucicutia hulsemannae*, closely related to the Arabian Sea LO copepod *L. grandis* (earlier literature called both species *L. grandis*). These copepods were restricted to this zone from the youngest copepodite stages to adults. Other abundant ETNP calanoids of the LO community included *Heterostylites longicornis*, *Pleuromamma johnsoni*, and *Metridia brevicauda*, but these taxa had wider distributions in the upper ocean for some stages. Small non-calanoid copepods were rare at these hypoxic levels in the ETNP similar to the Arabian Sea. Larger signature taxa included the shrimp *Gennadas* spp. and the fish *Cyclothone* spp. Planktonic foraminifera showed a secondary peak in this zone, as did pelagic polychaetes, ostracods, and amphipods. Gelatinous animals and larger fish were occasionally caught but not quantitatively sampled. LO zooplankton did not show DVM; for most zooplankton (in this size range), DVM was restricted to the UO and OM.

3.9. *OMZ-related copepod life history strategy*

The common ETNP copepod *E. inermis* had a life history strategy that strongly interacted with OMZ hydrography, with apparent ontogenetic vertical descent and longterm residence at the upper and lower boundaries of the OMZ (Fig. 10, Table 7). The LO *Eucalanus* layer, comprised mostly of adult females and male C5 life history stages, was positioned either overlapping with or slightly shallower than the normal LO zooplankton assemblage, and at even lower oxygen concentration. It varied in depth between years and stations along with the LO community. Many animals in this layer had stored oil, and at least some females contained developing eggs. Additionally, a smaller peak of *E. inermis* females occurred at the upper edge of the OMZ (300–350 or 200–300 m) at the CRD station each year but was not evident at TB. The UO *Eucalanus* layer occurred at about the same oxygen level, but higher temperature (11 °C vs. 7 °C), than the LO *Eucalanus* layer (Table 7). At the TB station both years, a high abundance of young stages (C1, C2, and other immature stages) at the thermocline indicated recent reproduction. Development apparently occurred in the upper water column, with mixed life history stages found there, including females with eggs. These animals lived at much higher temperatures and oxygen levels than their relatives at depth.

3.10. *OMZ expansion: A natural experiment*

Spatial and temporal variability between the two stations in depth and thickness of the OM and other ecological zones provided a natural experiment with regard to possible effects of future OMZ expansion (Fig. 2, Table 2). In 2007, the OM depth range was similar at both stations (~350–550 m); however, in 2008, OM range and thickness varied substantially between locations, extending from 80 to 700 m at TB but only 300–500 m at CRD. As a consequence, during 2008 at TB, much of the euphotic zone, including the deep chlorophyll maximum, was below the ML within the lowest oxygen water of the OM. The UO was substantially thicker in 2007 at both stations (20–350 m) and in 2008 at CRD (20–300 m), compared to the very thin UO (40–80 m) in 2008 at TB. The lowest oxygen habitat, therefore, began much shallower in the water column at TB versus CRD in 2008, and in comparison to 2007, and extended much deeper.

There were several biological consequences associated with hydrographic differences between stations in 2008 (Fig. 11). The same biomass features were present at both locations but responded differently to changes in OMZ thickness and boundary depths (Figs. 5 and 11, Table 7). The thermocline, at the upper OMZ boundary, was the location of peak zooplankton biomass at both locations, regardless of OMZ depth and extent. The LO biomass peak at the lower OMZ boundary appeared to be strongly locked into position by oxygen concentration. In 2008, it changed depth by over 200 m between stations (775–800 m at TB with its thick OMZ versus 525–550 m at CRD), as well as showing a temperature difference of ~2 °C between locations (5.7 °C versus 7.5 °C, respectively). However, the oxygen concentration at the two depths where this layer was located was virtually identical at both stations (~2 μM).

In contrast, for animals within the UO, the depth (and temperature at that depth) of the daytime DVM peak was similar at the two stations (200–300 m, 11.0–11.9 °C), even though oxygen concentration was substantially lower at TB than at CRD (1.3 μM versus 6.2 μM) (Fig. 11, Table 7). Thus, on a daily basis, animals (total biomass) at these two stations migrated to a nearly constant depth (within the hundred meter range of adjacent net strata), regardless of oxygen concentration.

There were differences among size fractions in response to the spatial hydrographic variability, however (Fig. 6, Table 4A). The percentage vertical distribution of biomass by ecological and depth zones differed strongly between locations in 2008 and in comparison with 2007. In 2008, when the OM at TB began at only

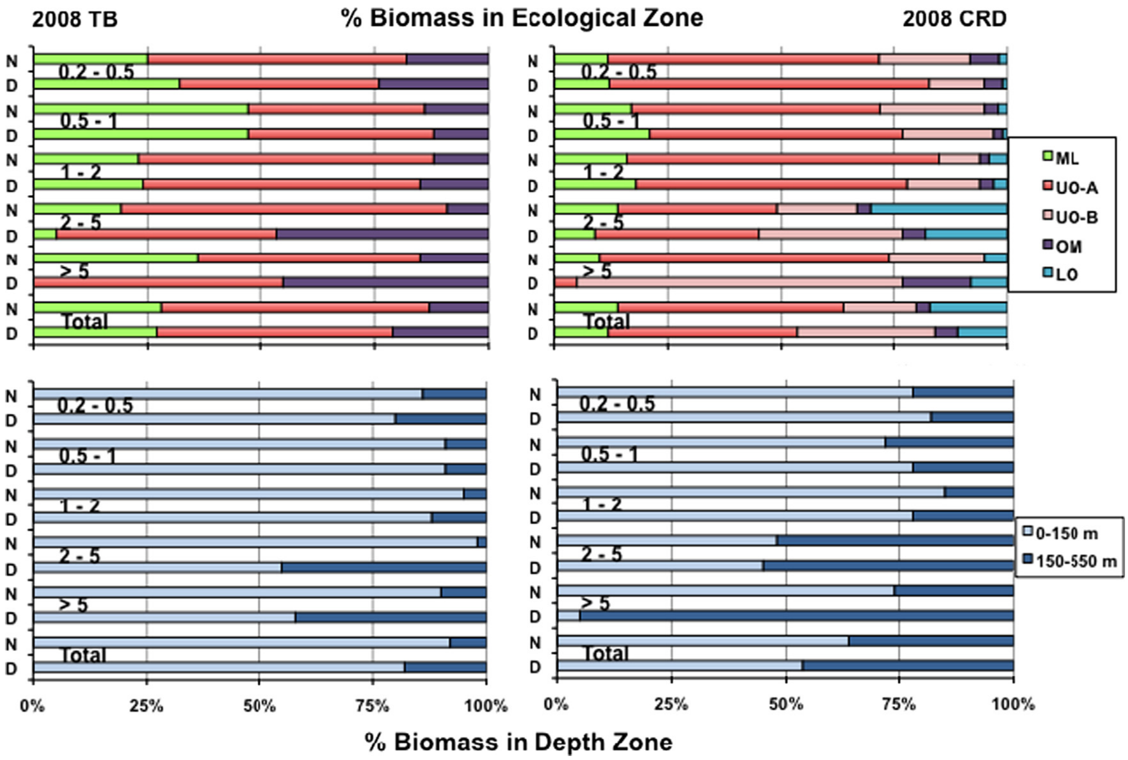

Fig. 6. Cumulative percent bar graphs showing biomass distribution differences between the two stations in 2008, when OMZ thickness varied substantially between locations. Graphs show the percent of water column biomass (0—550 m) for each size class and for total biomass night (N) and day (D). In each graph, the smallest size class is shown in the two uppermost bars (paired night and day). Larger size classes are paired sequentially down each graph, with total biomass shown in the two lowest bars. Numbers at the left indicate size class for each pair of bars. Top graphs show the % of 0—550 m biomass in each ecological zone (see Table 2 for abbreviations). Bottom graphs show the % of 0—550 m biomass in each depth zone. TB graphs are on the left; CRD graphs are on the right. See Tables 3 and 4A for biomass values.

80 m depth, a higher percentage of all size fractions was restricted to the upper 150 m there compared to the other situations, a quantifiable measure of the impact of habitat compression. This suggested that the expanded OM was a partial barrier to many organisms, restricting the depth of their distributions. However, 26% of the water column biomass for the smallest size class and 13% for the next size class did occur in this lowest oxygen environment (the OM) at TB in 2008 (but mostly within the upper 150 m), compared to a mean of only 4% ± 2 at CRD in 2008 and at both stations in 2007. DVM into the OM still occurred at TB in 2008, especially for larger (> 2 mm) taxa. To summarize, when the ML and UO were substantially limited in vertical extent by OM expansion up to shallower depths (at TB), some of the smaller taxa that normally did not reside in the lowest oxygen OM water now occurred there, although their depth range was reduced; larger migrators were less affected, with DVM continuing to occur to several hundred meters.

4. Discussion

4.1. Sampling issues

The 25-m sampling resolution and shipboard control of MOCNESS tows with simultaneous rapid response oxygen measurements, as well as adaptive sampling of zooplankton layers, enabled identification of fine-scale distributional associations with specific oxygen concentrations that eluded most earlier studies. These layers are not at a fixed depth but track particular oxyclines, whose depth may vary spatially and temporally. Net intervals based on a prior CTD will often miss or muddle the zooplankton layering. Although we were able to isolate the LO community within a single 25 m net interval (that varied in depth between years and stations), species distributions are probably much more compact, multi-layered, and precisely associated with specific environmental features and oxygen levels. Documenting these finer-scale distributional patterns requires other sampling instruments.

This study did not address mechanisms causing changes in OMZ extent. The increase in OMZ thickness at TB from 2007 to 2008 was most likely due to advection of more low oxygen water, possibly associated with ENSO phase (Arntz et al., 2006; Chavez and Messié, 2009). It was far too short a time to be a result of global climatic OMZ expansion. However, the serendipitous timing of the cruises and spatial comparisons between locations allowed us to separate effects of depth, temperature, and oxygen on zooplankton layer distributions in OMZs and to highlight potential consequences of future OMZ expansion.

4.2. Biomass patterns

The presence of an OMZ does not appear to strongly impact total 0–1000 m zooplankton biomass in a worldwide perspective, likely because much of that biomass is shallow. Geographic differences between stations, and comparisons with other world areas where zooplankton dry mass biomass was obtained with relatively similar size fractionation methods and MOCNESS nets, supported the importance of global surface productivity patterns in determining overall water column zooplankton biomass, regardless of the presence of an OMZ. The ETNP 0–1000 m biomass (34–145 mMC/m^2, 1214–5135 mg/m^2, Table 3) was generally within the range of biomass from the multiple stations and seasons of another productive strong OMZ region, the Arabian Sea (Wishner et al. 1998, 52–319 mMC/m^2), except for TB in 2007. The lower biomass there was similar to that of the oligotrophic subtropical Pacific (Steinberg et al., 2008a). CRD had higher biomass, supporting its history of being a productive habitat with

Table 5
Percent biomass change between night and day from paired profiles in each ecological zone and depth zone for each size fraction at the two stations and years. Values are the difference (night minus day) in percent of water column biomass in that zone. The depth range used is 0–1000 m in 2007 and 0–550 m in 2008, corresponding to the deepest extent of paired tows each year. Missing zones in 2008 are below the depth range covered. Positive numbers indicate higher % biomass during the night in that zone while negative values indicate higher % biomass during the day.

Station & Yr (depth range)	Zone	% Biomass change (Night–day)					
		Size fraction (mm)					
		Total	>5	2–5	1–2	0.5–1	0.2–0.5
TB 2007 (0–1000 m)	**ML**	9	0	19	−1	13	−1
	UO	14	45	−10	14	−8	6
	OM	−8	−27	−4	−3	0	−2
	LO	−10	−13	−5	−9	−5	−3
	SO	−5	−5	0	1	0	0
	0–150 m	27	9	32	22	9	8
	150–550	−12	9	−26	−13	−4	−5
	550–1000	−14	−18	−5	−9	−4	−3
CRD 2007 (0–1000 m)	**ML**	0	8	1	1	2	6
	UO	12	49	−3	−5	−5	−13
	OM	−2	−12	1	2	0	3
	LO	0	−3	0	3	3	3
	SO	−9	−41	−1	0	0	1
	0–150 m	26	81	14	5	−2	−6
	150–550	−16	−36	−14	−8	−2	2
	550–1000	−9	−45	−1	3	4	4
TB 2008 (0–550 m)	**ML**	1	36	14	−1	0	−7
	UO	7	−6	23	4	−2	13
	OM	−8	−30	−37	−3	2	−6
	0–150 m	10	32	43	7	0	6
	150–550	−10	−32	−43	−7	0	−6
CRD 2008 (0–550 m)	**ML**	2	10	5	−2	−4	1
	UO	−7	8	−15	2	2	−4
	OM	−2	−15	−2	−1	1	3
	LO	6	−3	12	1	1	1
	0–150 m	10	69	3	7	−6	−4
	150–550	−10	−69	−3	−7	6	4

extensive fisheries, but it was only about half that of the eutrophic subarctic Pacific (Steinberg et al. 2008a). Differences each year between the two ETNP stations were likely due to regional differences in primary productivity (Pennington et al., 2006). Differences between years were likely an ENSO effect; the 2007 cruise was during a strong La Niña while the 2008 cruise occurred during a weak La Niña/transition period (Wolter, 2012).

OMZs clearly affect vertical partitioning and layering of zooplankton biomass, with potential impacts on trophic transfer and particle processing. In the ETNP, biomass layers at the thermocline, UO, and LO were evident, as well as a zone of extremely low biomass within the OMZ core. A major advance of this study was resolving the vertical extent of the LO zooplankton biomass layer. This narrow feature, located within the 575–825 m depth interval, was well below the daytime depths of most vertical migrators (150–400 m) and the thermocline-associated biomass peak (narrow layer within the 20–80 m depth interval). LO zooplankton, present day and night, did not vertically migrate. The LO layer also marked the upper edge for many bathypelagic taxa. Previous sampling with broader intervals (Saltzman and Wishner, 1997a; Wishner et al., 1998) could not determine whether the LO layer was a true peak or merely the beginning of the increased biomass below the OMZ; finer-scale resolution in 2008 clearly delineated a sharp peak (Fig. 11). An order of magnitude jump in biomass just below the OMZ core at the start of the LO is apparently a signature feature of strong OMZs and is substantially different from vertical biomass structure in more oxygenated regions (Steinberg et al., 2008a).

Zooplankton biomass layers are often localized zones of high biological rates and activity. At mesopelagic depths, layers are likely responsible for much of the processing of sinking material and ultimately the amount and composition of carbon and particulates reaching the deep seafloor (Robinson et al., 2010). However, in OMZs, physiological reponses of zooplankton to low oxygen may modify the influence of layers. Pertinent adaptations include metabolic suppression and use of energetically inefficient anaerobic pathways (Seibel, 2011). Different species or taxa have different low oxygen tolerances and adaptations (examples from this project: Cass, 2011; Maas et al., 2012). The oxygen concentration in the ETNP OM is too low to support continuous aerobic metabolism in most organisms measured to date. Although adaptations for effective oxygen extraction characterize permanent residents of less pronounced OMZs (e.g. California Current: Childress and Seibel, 1998), species in the ETNP OM are at the apparent limit of oxygen extraction capacity (Seibel, 2011). Time spent in the OM should therefore be accompanied by behavior such as DVM to higher oxygen zones where the oxygen debt can be repaid; most (but not all) OM zooplankton biomass does migrate on a daily basis.

However, at the LO, where animals do not undergo DVM, they must be physiologically adapted for longterm residence in this extremely low oxygen habitat, intolerable for most taxa. We do not yet fully understand the physiology of small zooplankton, such as copepods, living continuously at low oxygen; measurements are needed of the critical oxygen partial pressure limiting metabolism at ambient conditions. Furthermore, precise measurement of small differences of in situ oxygen concentration at the very low oxygen levels and millimeter spatial scales occupied by individual zooplankters remains challenging (Thamdrup et al., 2012). It is also possible that LO animals undertake intermittent individual migration to deeper (rather than shallower) more oxygenated water. Oxyclines may form a fine-scale gradient of refuges for zooplankton, protecting more tolerant species from the bathypelagic predators of the SO.

Clearly, something other than oxygen concentration controlled the daytime depth of DVM into the UO, since that depth was remarkably similar at both ETNP stations despite a substantial difference in oxygen concentration (Table 7). The most likely candidates are light level, because of the presumed importance of low light for avoiding visual predators (Hays, 2003), and temperature, because of its effects on metabolic rates. Irradiance decreases exponentially with increasing depth and was probably similar at these two tropical ETNP stations, as was the vertical profile of temperature (Fig. 2). Other factors may also be important, and a constant DVM depth may not apply to all situations. For example, the predatory squid *Dosidicus gigas* migrates to different depths in the California Current versus Gulf of California, with its daytime depth at each location near its critical oxygen partial pressure (Stewart et al., in press; Trueblood and Seibel, in press). Also, use of the OMZ as a refuge from predators requiring higher oxygen would not explain why DVM penetrates so deeply into low oxygen water. Diel vertical migrators in OMZ regions cope with a much wider range of oxygen levels compared to migrators elsewhere, in order to reach their optimal daytime environment.

The horizontal and vertical distribution of size-fractionated zooplankton biomass is a fundamental attribute of oceanic ecosystems and a vital component of oceanic biogeochemical and global change models (e.g. Cheung et al., 2011; Décima et al., 2011). Zooplankton biomass directly affects the abundance of higher trophic level animals, such as fish that feed on zooplankton, and

Table 6
Similarities within Bray-Curtis clusters and *a priori* factor groups, and dissimilarities between each group pair, from ANOSIM and SIMPER tests. Asterisks indicate significant dissimilarity ($p < 0.05$). Global R values are also shown. See Table 2 for factor abbreviations.

Within-group similarity							
Sample group	**Avg similarity**	**Ox zone**	**Avg similarity**	**Depth zone**	**Avg similarity**	**Station**	**Avg similarity**
(63% slice)							
A	73.36	ML	78.57	Shallow	61.03	TB	50.34
B	74.69	UO	60.38	Mid	61.62	CRD	58.00
C	1 sample	OM	65.62	Deep	69.84		
D	79.46	LO	64.35				
E	73.01	SO	82.35				
F	73.55						
G	81.37						
Paired comparison dissimilarity							
Global R=0.851*	**Avg Dissim.**	Gl R=0.417*	**Avg Dissim.**	Gl R=0.455*	**Avg Dissim.**	Gl R=0.109*	**Avg Dissim.**
F, B	41.28*	UO, ML	40.81	S, D	60.29*	TB, CRD	49.69*
F, A	62.30*	UO, SO	57.77*	S, M	55.32*		
B, A	42.20*	ML, SO	73.92*	D, M	38.63*		
F, D	39.82*	UO, LO	52.31*				
B, D	64.76*	ML, LO	67.82*				
A, D	77.91*	SO, LO	31.22				
F, G	38.48*	UO, OM	55.43*				
B, G	52.16*	ML, OM	68.07*				
A, G	72.80*	SO, OM	39.53*				
D, G	40.14*	LO, OM	40.23*				
F, E	60.30*						
B, E	77.80*						
A, E	87.48*						
D, E	40.00*						
G, E	47.22*						
F, C	45.10*						
B, C	51.63*						
A, C	55.37*						
D, C	50.77						
G, C	50.78*						
E, C	65.56						

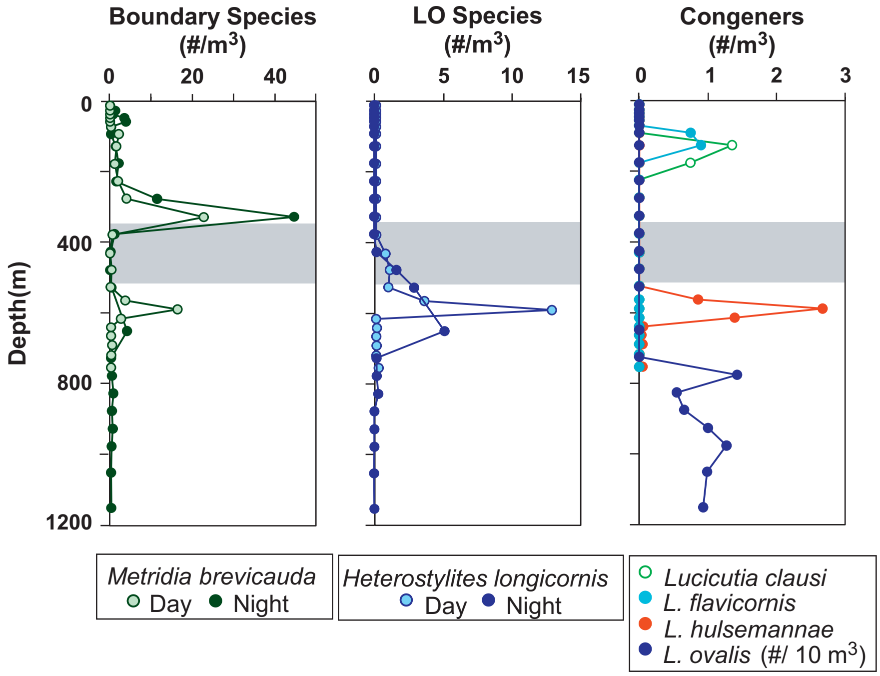

Fig. 7. Examples of different types of day and night vertical distributions for several copepod species (youngest identifiable copepodite stage to adults, CRD 2007). Only daytime distributions are shown for *Lucicutia* species for clarity, except for the deep-living *L. ovalis*, which is from a night tow (the day tow did not extend that deep). *L. ovalis* did not occur at shallower depths day or night. The gray box shows the OMZ core.

also likely controls much of the vertical flux of material to depth that results from zooplankton processing (Buesseler et al., 2008). Size fraction data, easier to obtain than species distributions, could be used to simplify models projecting consequences of potential OMZ expansion. In this study, sample groups defined only on the basis of biomass size composition showed OMZ zonation.

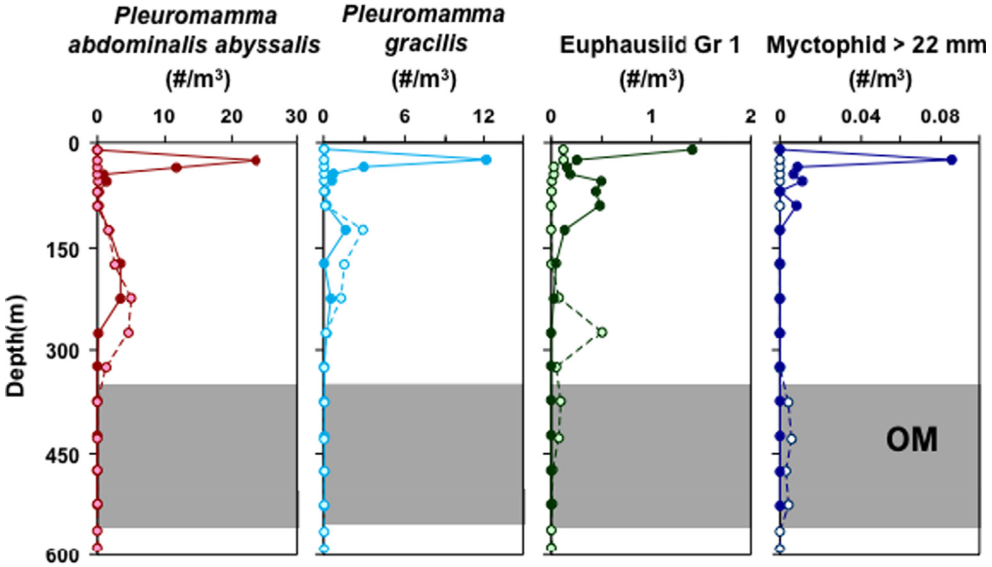

Fig. 8. Examples of diel vertical migration for several taxa (CRD 2007): two congeneric copepods (C2 to adults), a euphausiid group (mixed species with bi-lobed eyes), and a fish group. Day: open circles. Night: closed circles. The gray box is the OMZ core.

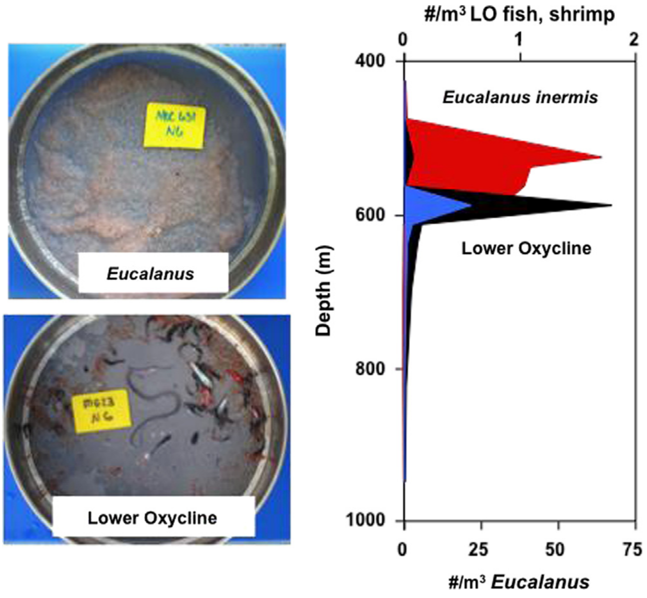

Fig. 9. Daytime abundances of two indicator taxa of the LO community, *Cyclothone spp*. fish (larger LO peak on the graph) and *Gennadas spp*. shrimp (smaller LO peak), along with the *Eucalanus inermis* copepod layer just above (stages C5 males and adult females, only stages present), showing the close vertical juxtaposition of these distinctive assemblages (CRD 2008). Photographs on the left show fresh samples representative of each habitat (tow 631 top photo, tow 623 bottom photo).

4.3. Zooplankton community structure and species distributions

Although many studies have documented distributions and adaptations of pelagic fauna in the California Current OMZ (e.g. Thuesen et al., 1998; Childress and Seibel, 1998; Seibel and Drazen, 2007; Robison et al., 2010), a key difference between that region and our site is the much lower oxygen concentration in the ETNP OMZ (~1.8 μM vs. ~10 μM off Monterey, CA). The permanent LO zooplankton community in the ETNP resides at an oxygen concentration of ~2 μM. A similar community occurs in the Arabian Sea LO but has not been reported from episodic oceanic "dead zones" off Oregon, in the Gulf of Mexico, or in coastal hypoxia events (Chan et al., 2008; Pierson et al., 2009; Zhang et al., 2009; Kimmel et al., 2010). Thus, it appears that a longterm oxygen gradient through this concentration range in the mesopelagic open ocean is the required habitat of the distinctive LO species assemblage.

The basic vertical distribution and ontogenetic migration of the copepod *E. inermis* was previously reported (Saltzman and Wishner, 1997b; Hidalgo et al., 2005; Escribano et al., 2009), but its precise positioning relative to the LO was unclear until this study. Earlier reports of narrow layers of *Eucalanus* in the lower ETNP OMZ from Longhurst-Hardy Plankton Recorder collections (Longhurst, 1967; 1976) and submersible observations (Vinogradov et al., 1991) occurred prior to widespread use of in situ electronic oxygen sensors, and thus could not resolve small-scale physical gradients. By sampling narrow depth intervals while filtering large volumes necessary for quantifying abundances and in conjunction with continuous environmental sensing, our work illuminated the interplay of oxygen, depth, and presumed predator avoidance in the life history strategy of this species, that facilitates its survival over time in this region.

Physiological studies of *E. inermis* from shallower depths showed metabolic suppression at low oxygen (Cass, 2011), but adaptations during its long residence in even lower oxygen at the LO remain a mystery. It was unclear whether individuals in the LO or UO layers were diapausing (Longhurst, 1976) although most had stored oil. In the layer just above the OM near 300 m (where oxygen values were generally similar to the LO layer, Table 7), lipid biomarkers indicated feeding on surface particles (Cass, 2011). Biogeographically, this species is uniquely adapted to inhabiting the ETNP with its strong but predictable environmental gradients (*sensu* McGowan, 1974), although its seasonal cycle in the ETNP has not yet been fully resolved because of sampling gaps.

LO and UO zooplankton seem to be active members of mesopelagic food webs, and zooplankton layers may be "hotspots" within the comparatively sparse midwater realm. OMZ zooplankton layers were sometimes coincident with layers of smaller particles or organisms, detected with the MOCNESS transmissometer, a towed camera system, lipid biomarkers from in situ pump samples (Rush et al., 2012), microbial molecular signatures from water samples (Podlaska et al., 2012), or microplankton microscopy (Olson and Daly, 2013). These items, presumably part of an active deep-sea microbial loop community, likely serve as food resources for mesopelagic zooplankton (Gowing et al., 2003).

Table 7
Hydrographic data from MOCNESS tows for sampling intervals where biomass peaks and selected species peaks were present for each station and year: the thermocline, the depth of daytime DVM at the base of the UO (or the peak *Eucalanus inermis* abundance in that zone), and the LO. The "LO community" was defined as the peak in abundance of *Lucicutia hulsemannae*. The LO biomass peak was also an *E. inermis* abundance peak. Ranges and tow means are shown. Temperature and oxygen data were binned by meter, then averaged. Data come from the upcast portion of the tow when the zooplankton samples were collected, except when noted. In a few cases, oxygen data from a nearby tow or CTD cast were used when the MOCNESS oxygen sensor failed.

Type of layer **Year Station**	**Tow & Net**	**Depth (m)** Range	**Temp (°C)** Range (tow means)	**Ox (μM)** Range (tow means)
Biomass (B)				
B-Thermocline				
2007 TB	608 N8, 609 N8	0–20	26.0–27.5 (27.5)	129.3-[b]200.1 ([b]199.2, 165.8)
2007 CRD	618 N7, 621 N7	20–30	15.6–26.7 (16.7, 23.0)	[c]46.3–125.2 (59.6, 89.6) (CTD)
2008 TB	626 N4, 633 N3	50–60, 60–80	15.0–20.8 (19.3, 17.4)	1.3–35.7 (21.4, 7.2)
2008 CRD	635 N7, 638 N7	20–30	17.7–24.4 (24.1, 20.0)	45.2–153.2 (145.2, 85.9)
B-Upper oxycline base (Day DVM)				
2007 TB	608 N5	[a]150–350	9.5–12.2 (10.9)	[b]1.0–3.1 (1.4)
2007 CRD	614 N5	[a]150–350	9.9–12.8 (11.4)	1.2–24.3 (8.3)
2008 TB	630 N6	250–300	10.8–11.3 (11.0)	[c]1.2–1.4 (1.3)
2008 CRD	637 N7	200–250	11.7–12.1 (11.9)	2.2–16.2 (6.2)
B-Lower oxycline				
2007 TB	608 N2, 609 N2	[a]750–900	5.1–5.9 (5.5, 5.4)	1.8–7.2 ([b]4.3, 4.5)
2007 CRD	617 N3, 614 N2	[a]550–750, [a]750–900	4.9–7.4 (6.5, 5.3)	1.1–15.0 (3.6, 7.1)
2008 TB (also E-LO)	631 N6	775–800	5.6–5.8 (5.7)	1.4–1.9 (1.7)
2008 CRD (also E-LO)	636 N8	525–550	7.4–7.7 (7.5)	1.4–2.4 (1.7)
LO Community				
2007 CRD	623 N7	575–600	6.5–6.5 (6.5)	1.3–2.0 (2.0)
2008 TB	631 N5	800–825	5.5–5.6 (5.6)	1.8–2.4 (2.1)
2008 CRD	636 N6	575–600	6.9–7.2 (7.1)	1.7–2.6 (2.1)
***Eucalanus inermis* (E)**				
E-Thermocline				
2007 TB	607 N7	20–80	13.5–27.4 (17.5)	3.0–200.8 (67.4)
2007 CRD	618 N6	30–40	14.7–15.4 (14.9)	[c]31.0–43.7 (35.8) (CTD)
2007 CRD	621 N6	30–40	15.6–17.3 (16.3)	[c]37.1–63.8 (49.7) (CTD)
2008 TB	626 N3	60–80	14.4–16.9 (15.4)	1.3–2.0 (1.4)
2008 TB	633 N3	60–80	15.0–19.5 (17.4)	1.3–20.5 (7.2)
2008 CRD	635 N3	60–80	13.7–14.8 (14.1)	15.9–31.9 (23.1)
2008 CRD	638 N6	30–40	15.3–17.6 (16.3)	40.6–47.0 (44.3)
E-Upper oxycline				
2007 CRD	615 N5	300–350	10.1–10.8 (10.5)	1.2–1.6 (1.4)
2007 CRD	616 N5	300–350	10.0–10.8 (10.3)	1.0–5.7 (2.7)
2008 CRD	637 N7	200–250	11.7–12.2 (11.9)	2.2–16.2 (6.2)
2008 CRD	641 N7	250–300	10.9–11.6 (11.3)	1.3–2.2 (1.5)
E-Lower oxycline				
2007 CRD	623 N7	575–600	6.5–6.5 (6.5)	1.3–2.0 (2.0)
2008 TB	632 N5	800–825	5.5–5.7 (5.6)	1.6–2.8 (2.1)
2008 CRD	637 N1	500–550	7.2–7.6 (7.4)	1.5–2.7 (2.1)

[a] Broad net interval.
[b] Downcast data.
[c] Another tow or CTD.

Although there is evidence for a variety of microbial production pathways (including chemoautotrophy) in strong oxyclines (e.g. Taylor et al., 2001; Voss et al., 2001; Lam et al., 2009; Molina and Farias, 2009; Kalvelage et al., 2011; Stewart F.J. et al., 2012; Wakeham et al., 2012), trophic transfer to zooplankton remains uncertain.

Stable isotopes (δ^{15}N of mixed zooplankton from these tows) showed virtually no change with depth through the OM but had an abrupt strong increase at the LO beginning at the depth of the zooplankton biomass peak (Fig. 11). An increasing gradient in δ^{15}N is often used as an indicator of a feeding progression to higher trophic levels (Fry, 2006). The vertical juxtaposition of isotope and biomass features suggested that the LO was a zone of increased in situ zooplankton feeding up the trophic web. This supported earlier studies of LO zooplankton feeding from gut content analyses (Gowing and Wishner, 1992, 1998) and in situ experiments (Wishner et al., 1995).

4.4. Consequences of OMZ expansion

A likely consequence of OMZ expansion is a change in the vertical distribution of zooplankton biomass layers, size classes, and species, with potential effects on food webs, particle fluxes, and biogeochemical cycles. This would affect ecosystem structure and function, including fisheries. Both shallow and mesopelagic zooplankton communities and biological pump processes are vulnerable to these changes, and there are also potential consequences for benthic–pelagic coupling. The most obvious example of a likely distributional shift, demonstrated as a spatial difference between stations, was the vertical re-positioning of zooplankton biomass layers at the thermocline and LO, the upper and lower OMZ boundaries, when confronted with different OMZ thicknesses (Figs. 5 and 12). At the thermocline boundary with an expanded OMZ, species tracking oxygen or constrained by temperature would be forced shallower (where there is more light) or

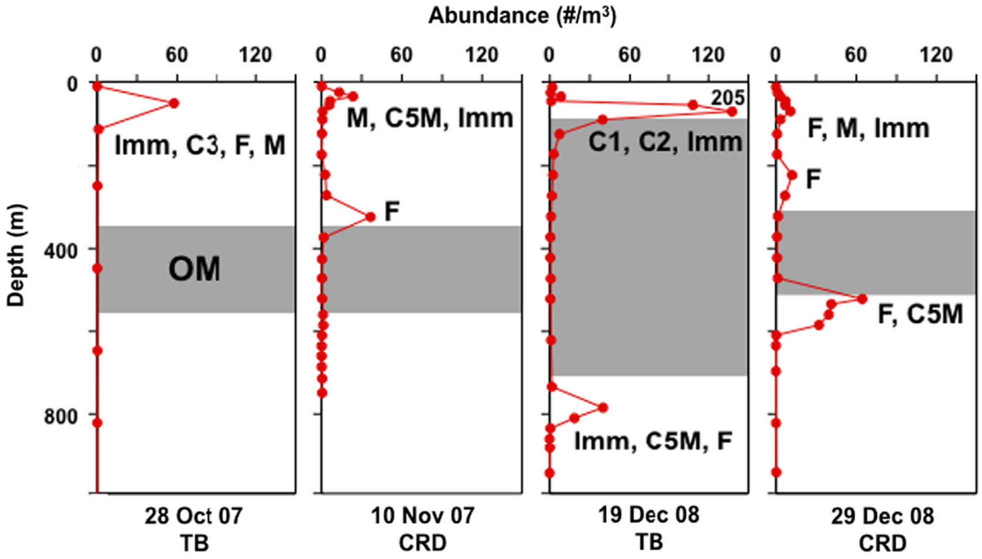

Fig. 10. Vertical profiles of *E. inermis* daytime distributions at each station each year to show the spatial and temporal variability in abundance peaks at the upper and lower OMZ boundaries. Points are summed abundances of life history stages C3 to adult. Labels list the most abundant stages (younger stages C1 and C2 are listed but not graphed). Imm=immatures stages C1—C5. The gray box represents the OMZ core.

compressed into narrower vertical zonation as the UO thins, with potentially more encounters with competitors and predators. Confirmation of this habitat compression effect in 2008 was the occurrence within the upper 150 m of 82% of zooplankton biomass at TB with its thick OMZ, compared to only 54% at CRD (0–550 m biomass, Table 3, Fig. 6). On the short term, this forced aggregation could benefit large epipelagic predators, making it easier for them to find food and possibly enhancing fisheries, but over time, with no physical refuge, zooplankton populations and the predators that depend on them would likely decline.

Several recent studies addressed fisheries implications of OMZ habitat compression and other changes. Bertrand et al. (2010) showed depth variability of acoustic targets associated with the upper OMZ boundary in the eastern South Pacific. Koslow et al. (2011) documented cyclical changes in mesopelagic fish abundance in the California Current OMZ. Stramma et al. (2011) showed decreased diving depths in large predatory fish associated with expanding hypoxia in the Atlantic. Although their interpretations focused on oxygen limitation for predators, an equally plausible explanation is shoaling of prey populations that relieves predators from deep-diving requirements. These fishery effects are all likely linked to zooplankton prey availability, especially the vertical position and intensity of the upper OMZ zooplankton boundary layer.

At the LO, species would be forced deeper to remain in their preferred oxygen habitat, perhaps beyond their pressure tolerance and at lower ambient temperature, likely reducing their metabolism (Figs. 5 and 12). This could affect feeding rates and the impact of the LO layer on particle processing (Wilson et al., 2008). The shift in depth of the δ^{15}N gradient (Fig. 11), a potential proxy for trophic progression (feeding up the food web), also suggests that the depth of zooplankton particle processing would change. Whether a deeper location would result in higher fluxes to depth because of less feeding on sinking material or lower fluxes because of less mesopelagic repackaging into dense fecal pellets is unknown. Syntheses of the extensive JGOFS POC flux dataset (0–5000 m) from four world regions suggested the possibility of differences in some curve parameters of Arabian Sea vertical flux profiles compared to more oxygenated locations, but both technical questions and interpretation issues remained (Berelson, 2001).

For diel vertical migrators, there is probably an interaction between a depth requirement and oxygen concentration in determining vertical position. If daytime DVM depth remains unaltered in an expanded OMZ, as our spatial comparison suggests, animals would then be exposed to lower oxygen for a greater time and distance. Some species might be physiologically unable to do the longer transit through hypoxic water. If the biomass of vertical migrators decreases, active vertical transport of carbon would likely diminish. Furthermore, metabolic suppression at low oxygen of ~35% below expected temperature-dependent respiration levels was documented for several species on this cruise (Cass, 2011; Maas et al., 2012; Seibel, 2011). Widespread metabolic suppression among OMZ zooplankton would further reduce the vertical flux of carbon via respiration (Steinberg et al., 2008b; Burd et al., 2010).

Within the OM where zooplankton biomass is extremely low, sinking particles may be subjected primarily to microbial decomposition until the particles reach the LO zooplankton layer, where they would encounter a gauntlet of animals that are active trophic processors. Thus, in locations with strong OMZs, much of the biological pump processing likely occurs in the deep mesopelagic at the base of the OMZ and in a more focused layer, compared to other oceanic regions. Although many unusual microbial processes occur in OMZs, it is not yet clear what effect a broader expanse of low oxygen water would have on overall particle decomposition rates and vertical fluxes. In the mesopelagic Arabian Sea during JGOFS, deeper sediment traps sometimes had higher flux values than shallower ones, a phenomenon attributed to lateral advection or methodological differences in trapping efficiency (Lee et al., 1998). Mesopelagic trophic repackaging, especially at the LO, is also a plausible explanation particularly in OMZ regions (Wishner et al., 2008).

Biogeographic changes might also occur. “Boundary” species, such as *M. brevicauda,* might have shallow and deep populations too widely separated by a thick OMZ to successfully transit that zone and interact effectively. The life history strategy of *E. inermis* might be disrupted, perhaps affecting mating, reproduction, and growth. Many of these zooplankton taxa are important food items for the abundant epipelagic fish and squid of the ETNP, and these fisheries could be adversely impacted.

Processes that affect mesopelagic zooplankton layer depths are likely to also alter benthic–pelagic coupling along continental shelves, seamounts, and submarine canyons. Where these OMZ-associated layers intersect the sea floor, they probably serve as

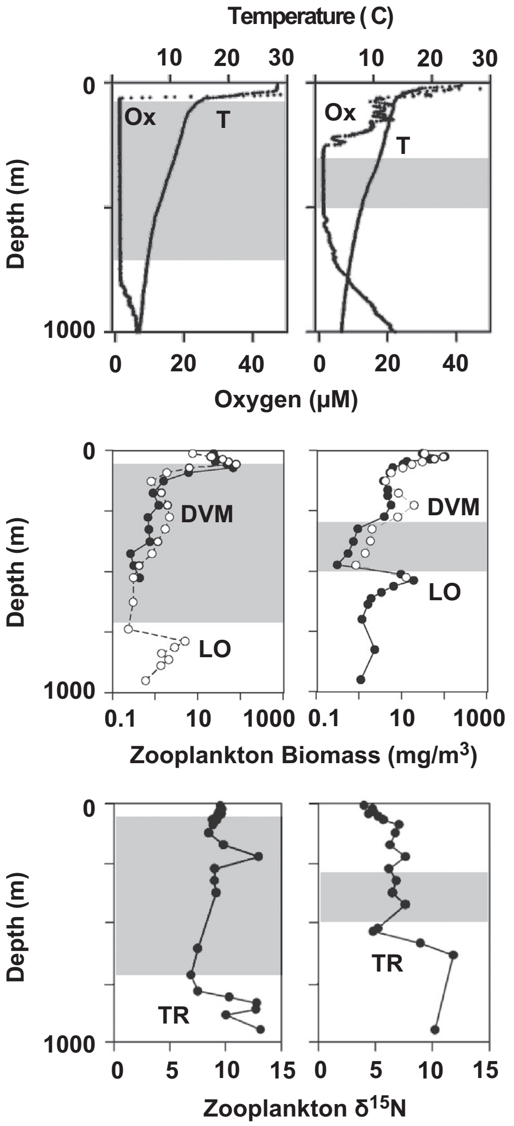

Fig. 11. Changes in depth of hydrographic and zooplankton features between the two stations in 2008, when OMZ thickness varied substantially between locations. Left side: station TB; right side: station CRD. Gray boxes represent the depth range of the OMZ core. Top: Hydrography (tow 632 from TB and 636 from CRD). Oxygen is offset slightly from the left axis for clarity and extends offscale at the surface. Middle: Day and night total zooplankton biomass on a logarithmic scale to highlight boundary layers. Night: closed circles; day: open circles. DVM = depth of daytime vertical migration. LO = lower oxycline layer. Bottom: Biomass-weighted mean stable isotope values from mixed zooplankton from these same tows and samples. TR = hypothesized zone of trophic progression up the food web (feeding) for the zooplankton community, inferred from the gradient of the δ^{15}N profile at the LO. Note the depth coincidence of the LO biomass layer and isotope gradient and their similar shift in depth between locations.

food sources for suspension-feeding benthos and demersal fish. Thus, changes in zooplankton layer depths in OMZs could affect food availability and alter benthic zonation (Wishner et al., 1990; 1995; Levin et al., 2003, 2009; Gallardo et al., 2004; De Leo et al., 2012).

5. Conclusions

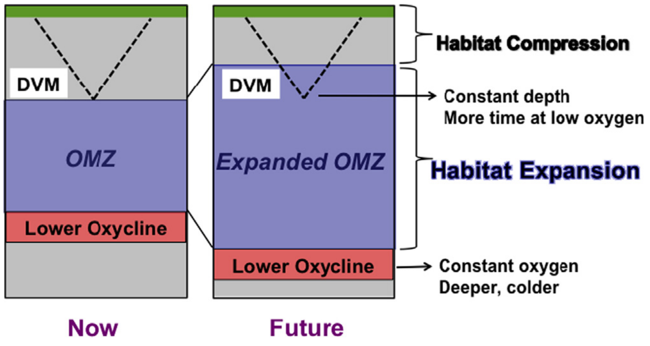

Fig. 12. Schematic scenario of OMZ expansion, showing predicted vertical re-positioning of biomass layers and potential consequences. The underlying diagram is modified from Seibel (2011).

The spatial comparison between the two stations (Tehuantepec Bowl and Costa Rica Dome), with different OMZ thicknesses, proved to be a useful proxy for possible future temporal change and revealed how variability in oxycline depth at the upper and lower OMZ boundaries could have broad consequences for biological distributions and ecosystem function (Fig. 12). The same biomass and distributional features, present at both locations, responded differently to changes in OMZ thickness and boundary depths. Peak zooplankton biomass occurred at the thermocline regardless of OMZ core depth, but two secondary mesopelagic biomass and abundance peaks showed very different responses to changes in oxygen vertical profiles between locations. The impact of habitat compression was quantified by the change in proportion of zooplankton biomass in the upper water column. Key findings include:

1. At the lower oxycline, a unique zooplankton assemblage and secondary biomass peak (sharp order of magnitude jump from OMZ biomass levels) occurred at an oxygen concentration of ~2 μM. The LO layer, strongly locked into position by oxygen concentration, changed depth by over 200 m between the two locations (775–800 m vs. 525–550 m, respectively) while remaining at the same oxygen level (but different temperature). The sharpness of the boundary between the OMZ core and LO layer, definition of its structure as a mesopelagic biomass peak rather than a continuous biomass increase with depth, and its precise association with a specific extremely low oxygen value, were important new findings from this work.
2. Quantification of the dense monospecific layer of the copepod *E. inermis*, sometimes present just above the regular LO assemblage, filled a gap in knowledge of this important species. While its general distribution and ontogenetic migration was previously known, its precise positioning relative to oxygen concentration and the LO community was a new discovery.
3. In contrast, the other secondary biomass peak, corresponding to the daytime depth of diel vertical migration and occurring within the upper oxycline or OMZ core, was present at the same depth (200–300 m) at both locations, despite different oxygen concentrations. If migrators must descend to this depth (to avoid predators, for example) through an expanded OMZ with an increased depth range of low oxygen, their longterm existence in the changing ocean of the ETNP might be compromised.

In summary, the vertical re-positioning of biomass layers at the thermocline and lower OMZ boundaries, and the increased depth range of low oxygen water that diel vertical migrators and sinking particles must transit in an expanded OMZ, could have widespread effects on species distributions, particle fluxes, the biological pump, and benthic–pelagic coupling.

Acknowledgements

We thank the captains, crews, and marine technicians of the R/V Seward Johnson and R/V Knorr and marine offices of HBOI and WHOI for productive cruises. E. Horgan, J. Lovin, and P. Wiebe provided MOCNESS technical assistance. Students N. Charriere, A. Cleary, S. Frazar, J. Graff, A. Maas, M. McNamara, M. O'Brien, J. Pelser, B. Phillips, J. Schneider, and K. Vogel helped with the MOCNESS project. C. Flagg made available processed CTD hydrographic data. B. Olson, A. Remsen, R. Sambrotto, G. Taylor, and S. Wakeham provided discussions and data. C. Cass, A. Maas, and A. Podlaska provided draft manuscripts. This project was funded by National Science Foundation grants OCE0526545 to Daly and OCE0526502 to Wishner and Seibel. The Graduate School of Oceanography's summer REU program, SURFO, funded S. Frazar (NSF grant OCE-0851794 to R. Pockalny). We also thank the University of Rhode Island for faculty and student funding.

References

Ashjian, C.J., Smith, S.L., Flagg, C.N., Idrisi, N., 2002. Distribution, annual cycle, and vertical migration of acoustically derived biomass in the Arabian Sea during 1994–1995. Deep Sea Res. Part II 49, 2377–2402.

Arntz, W.E., Gallardo, V.A., Guttiérrez, D., Isla, E., Levin, L.A., Mendo, J., Neira, C., Rowe, G.T., Tarazona, J., Wolff, M., 2006. El Niño and similar perturbation effects on the benthos of the Humboldt, California, and Benguela Current upwelling ecosystems. Adv. Geosci. 6, 243–265.

Baird, R.C., Wilson, D.F., Milliken, D.M., 1973. Observations on *Bregmaceros nectabanus* Whitley in anoxic, sulfurous water of Cariaco-Trench. Deep Sea Res. 20, 503–504.

Berelson, W.M., 2001. The flux of particulate organic carbon into the ocean interior: a comparison of four U.S. JGOFS regional studies. Oceanography 14, 59–67.

Bertrand, A., Ballón, M., Chaigneau, A., 2010. Acoustic observation of living organisms reveals the upper limit of the oxygen minimum zone. PLoS One 5, e10330.

Bograd, S.J., Castro, C.G., Di Lorenzo, E., Palacios, D.M., Bailey, H., Gilly, W., Chavez, F.P., 2008. Oxygen declines and the shoaling of the hypoxic boundary in the California Current. Geophys. Res. Lett. 35, L12607.

Brinton, E., 1979. Parameters relating to the distributions of planktonic organisms, especially euphausiids in the eastern tropical Pacific. Prog. Oceanogr. 8, 125–289.

Buesseler, K.O., Trull, T.W., Steinberg, D.K., Silver, M.W., Siegel, D.A., Saitoh, S.-I., Lamborg, C.H., Lam, P.J., Karl, D.M., Jiao, N.Z., Honda, M.C., Elskens, M., Dehairs, F., Brown, S.L., Boyd, P.W., Bishop, J.K.B., Bidigare, R.R., 2008. VERTIGO (VERtical Transport In the Global Ocean): a study of particle sources and flux attenuation in the North Pacific. Deep Sea Res. Part II 55, 1522–1539.

Burd, A.B., Hansell, D.A., Steinberg, D.K., Anderson, T.R., Arístegui, J., Baltar, F., Beaupré, S.R., Buesseler, K.O., DeHairs, F., Jackson, G.A., Kadko, D.C., Koppelmann, R., Lampitt, R.S., Nagata, T., Reinthaler, R., Robinson, C., Robison, B.H., Tamburini, C., Tanaka, T., 2010. Assessing the apparent imbalance between geochemical and biochemical indicators of meso- and bathypelagic biological activity: what the @$#! is wrong with present calculations of carbon budgets? Deep Sea Res. Part II 57, 1557–1571.

Cass, C.J., 2011. A Comparative Study of Eucalanoid Copepods Residing in Different Oxygen Environments in the Eastern Tropical North Pacific: An Emphasis on Physiology and Biochemistry. Ph.D. Thesis. University of South Florida, Tampa, FL., 165 pp.

Chan, F., Barth, J.A., Lubchenco, J., Kirincich, A., Weeks, H., Peterson, W.T., Menge, B. A., 2008. Emergence of anoxia in the California current large marine ecosystem. Science 319 920–920.

Chavez, F.P., Messié, M., 2009. A comparison of Eastern Boundary Upwelling Ecosystems. Prog. Oceanogr. 83, 80–96.

Chavez, F.P., Ryan, J., Lluch-Cota, S.E., Ñiquen, M., 2003. From anchovies to sardines and back: multidecadal changes in the Pacific Ocean. Science 299, 217–221.

Cheung, W.W.L., Dunne, J., Sarmiento, J.L., Pauly, D., 2011. Integrating ecophysiology and plankton dynamics into projected maximum fisheries catch potential under climate change in the Northeast Atlantic. ICES J. Mar. Sci. 68, 1008–1018.

Childress, J.J., Seibel, B.A., 1998. Life at stable low oxygen levels: adaptations of animals to oceanic oxygen minimum layers. J. Exp. Biol. 201, 1223–1232.

Clarke, K.R., Gorley, R.N., 2001. PRIMER v.5: User Manual/Tutorial. PRIMER-E Ltd., Plymouth, UK.

Diaz, R.J., Rosenberg, R., 2008. Spreading dead zones and consequences for marine ecosystems. Science 321, 926–929.

Danovaro, R., Dell'Anno, A., Pusceddu, A., Gambi, C., Heiner, I., Kristensen, R.M., 2010. The first metazoa living in permanently anoxic conditions. BMC Biol. 8, 30.

Décima, M., Landry, M.R., Rykaczewski, R.R., 2011. Broad scale patterns in mesozooplankton biomass and grazing in the eastern equatorial Pacific. Deep Sea Res. Part II 58, 387–399.

De Leo, F.C., Drazen, J.C., Vetter, E.W., Rowden, A.A., Smith, C.R., 2012. The effects of submarine canyons and the oxygen minimum zone on deep-sea fish assemblages off Hawai'i. Deep Sea Res. Part I 64, 54–70.

Deutsch, C., Brix, H., Ito, T., Frenzel, H., Thompson, L., 2011. Climate-forced variability of ocean hypoxia. Science 333, 336–339.

Ducklow, H.W., Steinberg, D.K., Buesseler, K.O., 2001. Upper ocean carbon export and the biological pump. Oceanography 14 (4), 50–58.

Ekau, W., Amel, H., Pörtner, H.O., Gilbert, D., 2010. Impacts of hypoxia on the structure and processes in pelagic communities (zooplankton, macro-invertebrates and fish). Biogeosciences 7, 1669–1699.

Escribano, R., Hidalgo, P., Krautz, C., 2009. Zooplankton associated with the oxygen minimum zone system in the northern upwelling region of Chile during March 2000. Deep Sea Res. Part II 56, 1049–1060.

Fernández-Älamo, M., Farber-Lorda, J., 2006. Zooplankton and the oceanography of the eastern tropical Pacific: a review. Prog. Oceanogr. 69, 318–359.

Fiedler, P., Talley, L., 2006. Hydrography of the eastern tropical Pacific: a review. Prog. Oceanogr. 69, 143–180.

Fiedler, P.C., 2002. The annual cycle and biological effects of the Costa Rica Dome. Deep Sea Res. Part I 49, 321–338.

Fry, B., 2006. Stable Isotope Ecology. Springer, NY.

Gallardo, V.A., Palma, M., Carrasco, F.D., Gutiérrez, D., Levin, L.A., Cañete, J.I., 2004. Macrobenthic zonation caused by the oxygen minimum zone on the shelf and slope off central Chile. Deep Sea Res. Part II 51, 2475–2490.

Gowing, M.M., Wishner, K.F., 1992. Feeding ecology of benthopelagic zooplankton on an eastern tropical Pacific seamount. Mar. Biol. 112, 451–467.

Gowing, M.M., Wishner, K.F., 1998. Feeding ecology of the copepod *Lucicutia aff. L. grandis* near the lower interface of the Arabian Sea oxygen minimum zone. Deep Sea Res. Part II 45, 2433–2459.

Gowing, M.M., Garrison, D.L., Wishner, K.F., Gelfman, C., 2003. Mesopelagic microplankton of the Arabian Sea. Deep Sea Res. Part I 50, 1205–1234.

Grantham, B.A., Chan, F., Nielsen, K.J., Fox, D.S., Barth, J.A., Huyer, A., Lubchenco, J., Menge, B.A., 2004. Upwelling-driven nearshore hypoxia signals ecosystem and oceanographic changes in the northeast Pacific. Nature 429, 749–754.

Haury, L.R., McGowan, J.A., Wiebe, P.H., 1978. Patterns and process in the time-space scales of plankton distributions. In: Steele, J. (Ed.) Spatial Patterns in Plankton Communities, Proceedings of the NATO Conference on Marine Biology, 1977, Plenum, NY, pp. 277–327.

Hays, G.C., 2003. A review of the adaptive significance and ecosystem consequences of zooplankton diel vertical migrations. Hydrobiology 503, 163–170.

Helly, J.J., Levin, L.A., 2004. Global distribution of naturally occurring marine hypoxia on continental margins. Deep Sea Res. Part I 51, 1159–1168.

Hidalgo, P., Escribano, R., Morales, C.E., 2005. Ontogenetic vertical distribution and diel migration of the copepod *Eucalanus inermis* in the oxygen minimum zone off northern Chile (20–21°S). J. Plankton Res. 27, 519–529.

Hidalgo, P., Escribano, R., Vergara, O., Jorquera, E., Donoso, K., Mendoza, P., 2010. Patterns of copepod diversity in the Chilean coastal upwelling system. Deep Sea Res. Part II 57, 2089–2097.

Hofmann, M., Schellnhuber, H., 2009. Oceanic acidification affects marine carbon pump and triggers extended marine oxygen holes. Proc. Nat. Acad. Sci. 106, 3017–3022.

Hunt, J.C., Seibel, B.A., 2000. Life history of *Gonatus onyx* (Cephalopoda: Teuthoidea): ontogenetic changes in habitat, behavior and physiology. Mar. Biol. 136, 543–552.

Kalvelage, T., Jensen, M.M., Contreras, S., Revsbech, N.P., Lam, P., Günter, M., LaRoche, J., Lavik, G., Kuypers, M.M.M., 2011. Oxygen sensitivity of anammox and coupled N-cycle processes in oxygen minimum zones. PLoS One 6 (e29299), 1–12.

Kamykowski, D., Zentara, S.J., 1990. Hypoxia in the world ocean as recorded in the historical data set. Deep Sea Res. Part A 37, 1861–1874.

Karstensen, J., Stramma, L., Visbeck, M., 2008. Oxygen minimum zones in the eastern tropical Atlantic and Pacific oceans. Prog. Oceanogr. 77, 331–350.

Keeling, R.F., Kortzinger, A., Gruber, N., 2010. Ocean deoxygenation in a warming world. Ann. Rev. Mar. Sci. 2, 199–229.

Kessler, W., 2006. The circulation of the eastern tropical Pacific: a review. Prog. Oceanogr. 69, 181–217.

Kimmel, D.G., Boicourt, W.C., Pierson, J.J., Roman, M.R., Zhang, X.S., 2010. The vertical distribution and diel variability of mesozooplankton biomass, abundance and size in response to hypoxia in the northern Gulf of Mexico USA. J. Plank. Res. 32, 1185–1202.

Koppelmann, R., Zimmermann-Timm, H., Weikert, H., 2005. Bacterial and zooplankton distribution in deep waters of the Arabian Sea. Deep Sea Res. Part I 52, 2184–2192.

Koslow, J.A., Goericke, R., Lara-Lopez, A., Watson, W., 2011. Impact of declining intermediate-water oxygen on deepwater fishes in the California Current. Mar. Ecol. Prog. Ser. 436, 207–218.

Lam, P., Lavik, G., Jensen, M.M., van de Vossenberg, J., Schmid, M., Woebken, D., Gutierrez, D., Amann, R., Jetten, M.S.M., Kuypers, M.M., 2009. Revising the nitrogen cycle in the Peruvian oxygen minimum zone. Proc. Nat. Acad. Sci. U.S.A. 106, 4752–4757.

Lee, C., Murray, D.W., Barber, R.T., Buesseler, K.O., Dymond, J., Hedges, J.I., Honjo, S., Manganini, S.J., Marra, J., Moser, C., Peterson, M.L., Press, W.L., Wakeham, S.G., 1998. Particulate organic carbon fluxes: compilation of results from the 1995 US JGOFS Arabian Sea Process Study. Deep Sea Res. Part II 45, 2489–2501.

Levin, L.A., 2003. Oxygen minimum zone benthos: adaptation and community response to hypoxia. Oceanogr. Mar. Biol. 41, 1–45.

Levin, L.A., Whitcraft, C.R., Mendoza, G.F., Gonzalez, J.P., Cowie, G., 2009. Oxygen and organic matter thresholds for benthic faunal activity on the Pakistan margin oxygen minimum zone (700–1100 m). Deep Sea Res. Part II 56, 449–471.

Longhurst, A., 1967. Vertical distribution of zooplankton in relation to eastern Pacific oxygen minimum. Deep Sea Res. 14, 51–63.

Longhurst, A.R., 1976. Interactions between zooplankton and phytoplankton profiles in the eastern tropical Pacific Ocean. Deep Sea Res. 23, 729–754.

Maas, A.E., Wishner, K.F., Seibel, B.A., 2012. Metabolic suppression in thecosomatous pteropods as an effect of low temperature and hypoxia in the eastern tropical north Pacific. Mar. Biol. 159, 1955–1967.

Martin, J.H., Knauer, G.A., Karl, D.M., Broenkow, W.W., 1987. VERTEX: carbon cycling in the northeast Pacific. Deep Sea Res. 34, 267–285.

McGowan, J.A., 1974. The nature of oceanic ecosystems. In: Miller, C.B. (Ed.), The Biology of the Oceanic Pacific. Oregon State Univ. Press, Corvallis, pp. 9–28.

Molina, V., Farias, L., 2009. Aerobic ammonium oxidation in the oxycline and oxygen minimum zone of the eastern tropical South Pacific off northern Chile (~20°S). Deep Sea Res. Part II 56, 1009–1018.

Morrison, J.M., Codispoti, L.A., Smith, S.L., Wishner, K., Flagg, C., Gardner, W.D., Gaurin, S., Naqvi, S.W.A., Manghnani, V., Prosperie, L., Gundersen, J.S., 1999. The oxygen minimum zone in the Arabian Sea during 1995. Deep Sea Res. Part II 46, 1903–1931.

Olson, M.B., Daly, K.L., 2013. Micro-grazer biomass, composition and distribution across prey resource and dissolved oxygen gradients in the far eastern tropical North Pacific Ocean. Deep Sea Res. Part I 75 (2013), 28–38.

Paulmier, A., Ruiz-Pino, D., 2009. Oxygen minimum zones (OMZs) in the modern ocean. Prog. Oceanogr. 80, 113–128.

Pennington, J.T., Mahoney, K.L., Kuwahara, V.S., Kolber, D.D., Calienes, R., Chavez, F.P., 2006. Primary production in the eastern tropical Pacific: a review. Prog. Oceanogr. 69, 285–317.

Pierson, J.J., Roman, M.R., Kimmel, D.G., Boicourt, W.C., Zhang, X.S., 2009. Quantifying changes in the vertical distribution of mesozooplankton in response to hypoxic bottom waters. J. Exp. Mar. Biol. Ecol. 381, S74–S79.

Podlaska, A., Wakeham, S.G., Fanning, K.A., Taylor, G.T., 2012. Microbial community structure and productivity in the oxygen minimum zone of the eastern tropical north Pacific. Deep Sea Res. Part I 66, 77–89.

Postel, L, Fock, H., Hagen, W., 2000. Biomass and abundance. In: Harris, R.P., et al. (Eds.), ICES Zooplankton Methodology Manual. Academic Press, San Diego, pp. 83–192.

Prince, E.D., Goodyear, C.P., 2006. Hypoxia-based habitat compression of tropical fishes. Fish. Oceanogr. 15, 451–464.

Rabalais, N.N., Diaz, R.J., Levin, L.A., Turner, R.E., Gilbert, D., Zhang, J., 2010. Dynamics and distribution of natural and human-caused hypoxia. Biogeosciences 7 (2), 585–619.

Robinson, C., Steinberg, D.K., Anderson, T.R., Aristegui, J., Carlson, C.A., Frost, J.R., Ghiglione, J.F., Hernandez-Leon, S., Jackson, G.A., Koppelmann, R., Queguiner, B., Ragueneau, O., Rassoulzadegan, F., Robison, B.H., Tamburini, C., Tanaka, T., Wishner, K.F., Zhang, J., 2010. Mesopelagic zone ecology and biogeochemistry—a synthesis. Deep Sea Res. Part II 57, 1504–1518.

Robison, B.H., Sherlock, R.E., Reisenbichler, K.R., 2010. The bathypelagic community of Monterey Canyon. Deep Sea Res. Part II 57, 1551–1556.

Rosa, R., Seibel, B.A., 2010. Metabolic physiology of the Humboldt Squid, *Dosidicus gigas*: implications for vertical migration in a pronounced oxygen minimum zone. Prog. Oceanogr. 86, 72–80.

Rush, D., Wakeham, S.G., Hopmans, E.C., Schouten, S., Damsté, J.S.S., 2012. Biomarker evidence for anammox in the oxygen minimum zone of the eastern tropical north Pacific. Org. Geochem. 53 (2012), 80–87.

Saltzman, J., Wishner, K.F., 1997a. Zooplankton ecology in the eastern tropical Pacific oxygen minimum zone above a seamount: 1. General trends. Deep Sea Res. Part I 44, 907–930.

Saltzman, J., Wishner, K.F., 1997b. Zooplankton ecology in the eastern tropical Pacific oxygen minimum zone above a seamount: 2. Vertical distribution of copepods. Deep Sea Res. Part I 44, 931–954.

Sameoto, D.D., 1986. Influence of the biological and physical environment on the vertical distribution of mesozooplankton and micronekton in the eastern tropical Pacific. Mar. Biol. 93, 263–279.

Seibel, B.A., 2011. Critical oxygen levels and metabolic suppression in oceanic oxygen minimum zones. J. Exp. Biol. 214, 326–336.

Seibel, B.A. The jumbo squid *Doscidicus gigas* (Ommastrephidae), living in oxygen minimum zones II: Blood-oxygen binding. Deep Sea Res. Part II., http://dx.doi.org/10.1016/j.dsr2.2012.10.003, in press.

Seibel, B.A., Drazen, J.C., 2007. The rates of metabolism in marine animals: environmental constraints, ecological demands and energetic opportunities. Philos. Trans. R. Soc. London, Ser. B 362, 2061–2078.

Smith, S., Madhupratap, M., 2005. Mesozooplankton of the Arabian Sea: patterns influenced by seasons, upwelling, and oxygen concentrations. Prog. Oceanogr. 65, 214–239.

Smith, S., Roman, M., Prusova, I., Wishner, K., Gowing, M., Codispoti, L.A., Barber, R., Marra, J., Flagg, C., 1998. Seasonal response of zooplankton to monsoonal reversals in the Arabian Sea. Deep Sea Res. Part II 45, 2369–2403.

Stanley, S.M., 2010. Relation of Phanerozoic stable isotope excursions to climate, bacterial metabolism, and major extinctions. Proc. Nat. Acad. Sci. U.S.A. 107, 19185–19189.

Steinberg, D.K., Cope, J.S., Wilson, S.E., Kobari, T., 2008a. A comparison of mesopelagic mesozooplankton community structure in the subtropical and subarctic North Pacific Ocean. Deep Sea Res. Part II 55, 1615–1635.

Steinberg, D.K., Van Mooy, B.A.S., Buesseler, K.O., Boyd, P.W., Kobari, T., Karl, D.M., 2008b. Bacterial vs. zooplankton control of sinking particle flux in the ocean's twilight zone. Limnol. Oceanogr. 53, 1327–1338.

Stewart, F.J., Ulloa, O., DeLong, E.F., 2012. Microbial metatranscriptomics in a permanent marine oxygen minimum zone. Environ. Microbiol. 14.1, 23–40.

Stewart, J.S., Field, J.C., Markaida, U., Gilly, W.F. Behavioral ecology of jumbo squid (*Dosidicus gigas*) in relation to oxygen minimum zones. Deep Sea Res. Part II, http://dx.doi.org/10.1016/j.dsr2.2012.06.005, in press.

Stramma, L., Johnson, G.C., Sprintall, J., Mohrholz, V., 2008. Expanding oxygen-minimum zones in the tropical oceans. Science 320, 655–658.

Stramma, L., Schmidtko, S., Levin, L.A., Johnson, G.C., 2010. Ocean oxygen minima expansions and their biological impacts. Deep Sea Res. Part I 57, 587–595.

Stramma, L., Prince, E.D., Schmidtko, S., Luo, J., Hoolihan, J.P., Visbeck, M., Wallace, D.W.R., Brandt, P., Körtzinger, A., 2011. Expansion of oxygen minimum zones may reduce available habitat for tropical pelagic fishes. Nat. Clim. Change 2, 33–37.

Taylor, G.T., Iabichella, M., Ho, T.-Y., Scranton, M.I., 2001. Chemoautotrophy in the redox transition zone of the Cariaco Basin: a significant midwater source of organic carbon production. Limnol. Oceanogr. 46, 148–163.

Taylor, G.T., Thunell, R., Varela, R., Benitez-Nelson, C., Scranton, M.I., 2009. Hydrolytic ectoenzyme activity associated with suspended and sinking organic particles within the anoxic Cariaco Basin. Deep Sea Res. Part I 56, 1266–1283.

Thamdrup, B., Dalsgaard, T., Revsbech, N.P., 2012. Widespread functional anoxia in the oxygen minimum zone of the eastern South Pacific. Deep Sea Res. Part I 65, 36–45.

Thuesen, E.V., Miller, C.B., Childress, J.J., 1998. Ecophysiological interpretation of oxygen consumption rates and enzymatic activities of deep-sea copepods. Mar. Ecol. Prog. Ser. 168, 95–107.

Trueblood, L.A., Seibel, B.A. The jumbo squid, *Dosidicus gigas* (Ommastrephidae), living in oxygen minimum zones I: Oxygen consumption rates and critical oxygen partial pressures. Deep Sea Res. Part II., http://dx.doi.org/10.1016/j.dsr2.2012.10.004, in press.

Utne-Palm, A.C., Salvanes, A.G.V., Currie, B., Kaartvedt, S., Nilsson, G.E., Braithwaite, V.A., Stecyk, J.A.W., Hundt, M., van der Bank, M., Flynn, B., Sandvik, G.K., Klevjer, T.A., Sweetman, A.K., Brüchert, V., Pittman, K., Peard, K.R., Lunde, I.G., Strandabø, R.A.U., Gibbons, M.J., 2010. Trophic structure and community stability in an overfished ecosystem. Science 329, 333–336.

Vinogradov, M.Y., Shuskina, E.A., Gorbunov, A.Y., Shaskov, N.L., 1991. Vertical distribution of the macro- and mesoplankton in the region of the Costa Rica Dome. Mar. Biol. 31, 559–565.

Voss, M., Dippner, J.W., Montoya, J.P., 2001. Nitrogen isotope patterns in the oxygen-deficient waters of the eastern tropical north Pacific Ocean. Deep Sea Res. Part I 48, 1905–1921.

Wakeham, S.G., Turich, C., Schubotz, F., Podlaska, A., Li, X.N., Varela, R., Astor, Y., Sáenz, J.P., Rush, D., Damsté, J.S.S., Summons, R.E., Scranton, M.I., Taylor, G.T., Hinrichs, K-U., 2012. Biomarkers, chemistry and microbiology show chemoautotrophy in a multilayer chemocline in the Cariaco Basin. Deep Sea Res. Part I 63, 133–156.

Ward, B.B., Tuit, C.B., Jayakamur, A., Rich, J.J., Moffett, J., Naqvi, S.W.A., 2008. Organic carbon, and not copper, controls denitrification in oxygen minimum zones of the ocean. Deep Sea Res. Part I 55, 1672–1683.

Wiebe, P.H., Boyd, S.H., Cox, J.L., 1975. Relationships between zooplankton displacement volume, wet weight, and carbon. Fish Bull. U.S. 73, 777–786.

Wiebe, P.H., 1988. Functional regression equations for zooplankton displacement volume, wet weight, dry weight, and carbon: a correction. Fish. Bull. U.S. 86, 833–835.

Wiebe, P.H., Morton, A.W., Bradley, A.M., Backus, R.H., Craddock, J.E., Barber, V., Cowles, T.J., Flierl, G.R., 1985. New developments in the MOCNESS, an apparatus for sampling zooplankton and micronekton. Mar. Biol. 87, 313–323.

Wilson, S.E., Steinberg, D.K., Buesseler, K.O., 2008. Changes in fecal pellet characteristics with depth as indicators of zooplankton repackaging of particles in the mesopelagic zone of the subtropical and subarctic North Pacific Ocean. Deep Sea Res. Part II 55, 1636–1647.

Wishner, K.F., Levin, L., Gowing, M., Mullineaux, L., 1990. Involvement of the oxygen minimum in benthic zonation on a deep seamount. Nature 346, 57–59.

Wishner, K.F., Ashjian, C.J., Gelfman, C., Gowing, M.M., Kann, L., Levin, L.A., Mullineaux, L.S., Saltzman, J., 1995. Pelagic and benthic ecology of the lower interface of the eastern tropical Pacific oxygen minimum zone. Deep Sea Res. Part I 42, 93–115.

Wishner, K.F., Gowing, M.M., Gelfman, C., 1998. Mesozooplankton biomass in the upper 1000 m in the Arabian Sea: overall seasonal and geographic patterns, and relationship to oxygen gradients. Deep Sea Res. Part II 45, 2405–2432.

Wishner, K.F., Gowing, M.M., Gelfman, C., 2000. Living in suboxia: ecology of an Arabian Sea oxygen minimum zone copepod. Limnol. Oceanogr. 45, 1576–1593.

Wishner, K.F., Gelfman, C., Gowing, M.M., Outram, D.M., Rapien, M., Williams, R.L., 2008. Vertical zonation and distributions of calanoid copepods through the lower oxycline of the Arabian Sea oxygen minimum zone. Prog. Oceanogr. 78, 163–191.

Wolter, K. Multivariate ENSO Index (MEI). Website of the Earth System Research Laboratory, NOAA, US Dept. of Commerce. URL: ⟨www.esri.noaa.gov/psd/enso/mei/#Home⟩ (accessed 11/16/12).

Zhang, H.Y., Ludsin, S.A., Mason, D.M., Adamack, A.T., Brandt, S.B., Zhang, X.S., Kimmel, D.G., Roman, M.R., Boicourt, W.C., 2009. Hypoxia-driven changes in the behavior and spatial distribution of pelagic fish and mesozooplankton in the northern Gulf of Mexico. J. Exp. Mar. Biol. Ecol. 381, 580–591.